AD-A196 877

REPORT DOCUMENTATION PAGE		READ INSTRUCTIONS BEFORE COMPLETING FORM
1. REPORT NUMBER AFIT/CI/NR 88- 59	2. GOVT ACCESSION NO.	3. RECIPIENT'S CATALOG NUMBER
4. TITLE *(and Subtitle)* NEUTRON MULTIPLICATION IN BERYLLIUM		5. TYPE OF REPORT & PERIOD COVERED MS THESIS
		6. PERFORMING ORG. REPORT NUMBER
7. AUTHOR(s) RICHARD STEVEN HARTLEY		8. CONTRACT OR GRANT NUMBER(s)
9. PERFORMING ORGANIZATION NAME AND ADDRESS AFIT STUDENT AT: UNIVERSITY OF TEXAS AT AUSTIN		10. PROGRAM ELEMENT, PROJECT, TASK AREA & WORK UNIT NUMBERS
11. CONTROLLING OFFICE NAME AND ADDRESS		12. REPORT DATE 1988
		13. NUMBER OF PAGES 158
14. MONITORING AGENCY NAME & ADDRESS*(if different from Controlling Office)* AFIT/NR Wright-Patterson AFB OH 45433-6583		15. SECURITY CLASS. *(of this report)* UNCLASSIFIED
		15a. DECLASSIFICATION/DOWNGRADING SCHEDULE

16. DISTRIBUTION STATEMENT *(of this Report)*

DISTRIBUTED UNLIMITED: APPROVED FOR PUBLIC RELEASE

17. DISTRIBUTION STATEMENT *(of the abstract entered in Block 20, if different from Report)*

SAME AS REPORT

18. SUPPLEMENTARY NOTES

Approved for Public Release: IAW AFR 190-1
LYNN E. WOLAVER 19/July 88
Dean for Research and Professional Development
Air Force Institute of Technology
Wright-Patterson AFB OH 45433-6583

19. KEY WORDS *(Continue on reverse side if necessary and identify by block number)*

20. ABSTRACT *(Continue on reverse side if necessary and identify by block number)*

ATTACHED

8

Integral neutron multiplication experiments have been performed using homogeneous spherical shells of beryllium metal of 4.6-, 6.99-, 7.87-, 9.38-, 13.8-, and 19.9-cm thickness. Neutron leakage, produced by Cf-252 and DT neutron sources placed in the center of the shells, were measured with a Bonner sphere spectrometer system. The rate of DT neutron production was normalized using an associated particle system placed inside the target assembly which was inserted into the shells via a reentrant hole.

The neutron fluence was obtained by processing the room-returned and air-scattered corrected count-rate data with a Bonner sphere spectrum unfolding routine and a weighted Bonner sphere technique. The neutron multiplication was obtained directly by comparing the normalized neutron leakage fluence with and without beryllium present.

The neutron leakage spectra were calculated for each shell using the discrete ordinates codes ANISN and ONEDANT using ENDF/B-IV and ENDF/B-V respectively. The cross sections from ENDF/B-V included the most current revisions from the Los Alamos National Laboratory. A comparison of the leakage multiplication, calculated using the two versions of evaluated nuclear data, indicate that corrections have been made to the energy-angle distribution of the secondary neutrons in ENDF/B-V resulting in a lower neutron leakage multiplication for shells greater than 9.38-cm thickness. The results indicate that the Los Alamos revisions to ENDF/B-V reduced the neutron leakage multiplication for the thicker shells resulting in calculations more closely aligned with experimental results.

> These Theses <

Availability Codes

Dist	Avail and/or Special
A-1	

NEUTRON MULTIPLICATION IN BERYLLIUM

by

RICHARD STEVEN HARTLEY, B.S., M.S.

CAPTAIN, USAF

158 pages

DISSERTATION

Presented to the Faculty of the Graduate School

The University of Texas at Austin

in Partial Fulfillment

of the Requirements

for the Degree of

DOCTOR OF PHILOSOPHY

THE UNIVERSITY OF TEXAS AT AUSTIN

1987

NEUTRON MULTIPLICATION IN BERYLLIUM

APPROVED BY

SUPERVISORY COMMITTEE:

TO MY CHILDREN

NEUTRON MULTIPLICATION IN BERYLLIUM

by

RICHARD STEVEN HARTLEY, B.S., M.S.

DISSERTATION

Presented to the Faculty of the Graduate School

The University of Texas at Austin

in Partial Fulfillment

of the Requirements

for the Degree of

DOCTOR OF PHILOSOPHY

THE UNIVERSITY OF TEXAS AT AUSTIN

December 1987

ACKNOWLEDGMENTS

iv

NEUTRON MULTIPLICATION IN BERYLLIUM

Publication No.

Richard Steven Hartley, Ph.D.

The University of Texas at Austin, 1987

Supervising Professor: Nolan E. Hertel

A technique of using a Bonner sphere spectrometer for testing integral cross sections has been developed. Integral neutron multiplication experiments using the technique have been performed using spherical shells of beryllium metal of 4.6 cm, 6.99 cm, 7.87 cm, 9.38 cm, 13.8 cm, and 19.9 cm thickness. Neutron leakage, from a ^{252}Cf and a DT neutron source normalized using the associated particle technique, were measured with a Bonner sphere spectrometer system.

The neutron fluence was obtained by processing the room-returned and air-scattered corrected count-rate data with a Bonner sphere spectrum unfolding routine. The neutron multiplication was obtained directly by comparing the normalized neutron leakage fluence with and without beryllium present.

A comparison of the leakage multiplication, calculated using ANISN with ENDF/B-IV and ONEDANT with ENDF/B-V with Los Alamos National Laboratory revisions (ENDF/B-V/LANL), indicate that in ENDF/B-V/LANL secondary neutrons are scattered preferentially in the

forward direction resulting in a lower neutron leakage multiplication
for thicker shells. The ENDF/B-V/LANL leakage multiplication for
^{252}Cf agrees with that predicted using ENDF/B-IV for thin shells
while predicting less than that using ENDF/B-IV for thicker shells
where the neutron energy is degraded below the (n,2n) threshold. The
DT leakage multiplication calculated using ENDF/B-V/LANL, while larger
than ENDF/B-IV for thin shells results in lower multiplication than
that using ENDF/B-IV for thick shells.

The measured ^{252}Cf neutron leakage multiplication agrees
with that calculated with ENDF/B-V/LANL although direct comparison
with the 13.8 cm and 19.9 cm assemblies, with missing hemispherical
shells, require multidimensional analyses.

The measured DT neutron leakage multiplication agrees well
with that calculated using ENDF/B-V/LANL for the 4.6 cm, 6.99 cm, and
7.87 cm thick shells. ENDF/B-V/LANL calculations indicate an increase
in the multiplication with beryllium thickness; whereas, the
measurements indicate a relatively flat response from 9.43 cm to 19.9
cm. The Los Alamos revisions to ENDF/B-V have reduced the neutron
leakage multiplication for the thicker shells resulting in
calculations more closely aligned with experimental results yet
further revisions may be indicated.

TABLE OF CONTENTS

Appendices

Chapter I Introduction

A.   The Need for Accurate Beryllium Multiplication Measurements

Self-sufficient fusion reactors using the deuterium-tritium fuel cycle require a tritium breeding ratio (TBR) greater than unity to provide the margin necessary to supply tritium inventory for new fusion reactors, to compensate for losses and radioactive decay between production and use, and to provide holdup inventory in various components as well as reserve storage inventory.[1] There is large uncertainty in this required margin due to the uncertainty involved in predicting the performance characteristics of the plasma such as:

1.   the efficiency of the burnup of tritium in the plasma,
2.   the amount of equilibrium inventories in the reactor components especially the blanket,
3.   the time required to attain equilibrium tritium inventories,
4.   the failure frequency of the tritium processing system,
5.   the processing efficiencies of various subsystems.

Likewise, the achievable TBR for a particular blanket design is also uncertain due to inaccuracies in predicting the TBR and

uncertainties associated with system definition (e.g., using a limiter versus divertor, nonbreeding inboard blanket in the tokamak, etc.).[2] The inaccuracies of predicting the TBR include uncertainties in the geometric modeling, the calculational methods, and the basic nuclear data.

Based solely upon the uncertainties in the nuclear data, the statistical relative standard deviation in the total TBR has been calculated to be 2.1% and 3.41% for the $LiAlO_2/H_2O/FS/Be$ and Flibe/He/HS/Be reactor designs, respectively.[2] The percent contribution from each blanket constituent to the uncertainty in tritium breeding by ^6Li and from ^7Li reactions for these two blanket concepts is shown in Table I.[2] The largest uncertainty (82% for $LiAlO_2$ and 88% for Flibe) results from the uncertainty associated with beryllium cross sections, in particular the uncertainties in the inelastic levels used to describe the $^9Be(n,2n)$ cross section in the Be-LANL evaluation.

B.   Integral Experiments

A technique for evaluating the adequacy of nuclear cross section data, held over from the testing of fission reactor core parameters, is to perform integral experiments to measure directly the effective neutron multiplication of beryllium.[3] The adequacy of evaluated nuclear data can be assessed by comparing experimental result with those predicted by proven calculational methods.[4] If

TABLE I

RELATIVE VARIANCE AND RSD IN THE TRITIUM BREEDING FROM

^{6}LI AND ^{7}LI AND THE TOTAL TBR DUE TO CROSS SECTION

UNCERTAINTIES OF VARIOUS METALS IN BLANKETS WITH BERYLLIUM[2]

ELEMENT	LiAlO$_2$/H$_2$O/FS/Be		Flibe/He/FS/Be	
	VARIANCE IN T6	VARIANCE IN T7	VARIANCE IN T6	VARIANCE IN T7
6Li	1.20-3	0.	3.82-2	0.
7Li	2.92-6	2.22+2	4.84-4	2.25+2
Oxygen	7.55-2	4.13	9.25-9	1.57-11
Iron	6.94-1	1.47+1	7.99-1	1.34
Nickel	1.49-12	2.79-12	4.09-8	1.27-12
Chromium				
Flourine			2.98-1	5.66
Silicon			7.31-2	4.75-1
Carbon			3.76-3	1.76-2
Hydrogen	1.51-3	9.89-2		
Aluminum	1.69-3	6.50-1		
Beryllium	3.54	9.30	9.77	9.91
TOTAL VARIANCE	4.31	2.51+2	1.10+1	2.42+2
RSD(%)	2.08	1.58+1	3.31	1.56+1
RSD IN THE TOTAL TBR(%)	+/- 2.1		+/-3.41	

T6 is the TBR from ^{6}LI.   T7 is the TBR from ^{7}LI.

RSD is the relative standard deviation.

a discrepancy results, it is narrowed to specific partial cross section data and the evaluations are investigated to discover inadequacies. The calculational methods are scrutinized to determine if the disagreement can be attributed to them. If the discrepancy is sensitive to partial cross sections, the calculated data can be adjusted within the experimental error to resolve the problem.

Previous integral beryllium neutron multiplication experiments[5,6] indicate that the basic nuclear data may overestimate the neutron multiplying properties of beryllium because of inadequate representation of the energy-angle distribution of the secondary neutrons.[7,8] An evaluation (Be-LANL) for the ^{9}Be cross sections has been updated to more correctly represent the energy-angle distribution from the ^{9}Be(n,2n) reactions.[2] There is a decrease in ^{9}Be(n,2n) reaction using the Be-LANL evaluation compared to that obtained using ENDF B-V. The decrease is due to the difference in the representation of the energy-angle distribution of the secondary neutrons rather than from the integrated value for the ^{9}Be(n,2n) cross section.

The decrease in neutron multiplication, with the total ^{9}Be(n,2n) cross section remaining the same for ENDF/B-IV,-V, and Be-LANL can be explained using the corrected energy-angle correlation. The correction made to the secondary neutron energy-angle correlations tend to transport the neutrons in the forward direction away from the breeding zone while ENDF/B-IV and -V

assumed isotropic scatter for the second neutron. Since the ^{9}Be(n,2n) reaction is the largest contributor to the excess neutrons, the relative number of neutrons available for further multiplication in the beryllium zone through successive (n,2n) reactions decreases. Therefore, the total number of neutrons available for breeding decreases in turn decreasing the TBR.

Although there are strong indications from previous integral experiments that the ^{9}Be(n,2n) cross section should be changed, it is not known by how much. Basu et al.[6] implied that the neutron multiplication in beryllium is overestimated by as much as 25%. This 25% deviation was thought to be due partly to deficiencies in the ^{9}Be(n,2n) cross-section evaluation and partly to the method used in analyzing the experiment.[2,9] For this reason, a direct integral measurement of beryllium multiplication is needed.

C.   Present Research

Bonner spheres, which are heavily used in health physics, have not yet been used in the integral tests of cross sections. The main emphasis of the present research was to develop, test, and use Bonner spheres to measure the neutron multiplication properties of beryllium. Several benchmark experiments were performed using polyethylene spheres as a proof-of-principle. The technique was then applied to determine neutron multiplication as a function of thickness

using spherical shells of beryllium obtained from the University of
Illinois (UI) and the Lawrence Livermore National Laboratory (LLNL).
The experiments were performed with a single material, in a simple
geometry utilizing well characterized sources, and with results
expressed in units that were independent of the detector. The tests
were performed by measuring neutron leakage from ^{252}Cf and DT
neutron sources placed inside the beryllium shells. The neutron
multiplication was determined directly by comparing the neutron
leakage from the spheres to bare source measurements. The neutron
spectra were measured using a Bonner sphere detector system
manufactured by Ludlum Measurements Inc.[10] The Bonner sphere
system, when the count-rates are properly weighted and summed,
provides a detection system which has a relatively constant detection
efficiency for all energies of interest. The neutron leakage was
determined by weighting the sums of observed Bonner-sphere counts and
by integrating crude energy spectra obtained by unfolding the same
Bonner sphere counts.

The present research was divided into tasks: correcting the
observed count-rate for the room-returned and air-scattered neutrons,
determining the angular distribution of the DT neutron sources,
measuring the multiplication for the available beryllium shells and
neutron sources, and calculating the multiplication using the most
current cross section sets available.

As a result of this research a technique of measuring

integral cross sections with Bonner spheres has been developed and tested. The technique provides a detector system with the ability to precisely measure neutron leakage spectra from thermal to 14 MeV. The use of a detector system with this extreme range of measurement capability allows integral experiments to be performed with a single detector system, simplifying the experiment and the resulting analyses.

Chapter II Beryllium: Uses, Evaluated Nuclear Data, and Integral Tests

A.   Uses of Beryllium in Fusion Reactors

A concise summary of the planned use of beryllium in fusion reactors can best be expressed by reviewing the Blanket Comparison and Selection Study (BCSS). The BCSS was a 2-yr, multilaboratory project initiated by the U.S. Department of Energy/Office of Fusion Energy to define a limited number of blanket concepts on which R&D efforts could be focused and to identify and prioritize critical issues for the leading blanket concepts.[1] The BCSS focused on the D-T-Li fuel cycle in tokamaks and tandem mirror reactors (TMRs) for electrical production with a parameter space that is considered achievable with modest extrapolations from the current data base. The STARFIRE and Mirror Advanced Reactor Study (MARS) reactor and plant designs with a nominal first-wall neutron loading of 5 MW/m^2 were used as the reference design for the study (Table II). Various blanket concepts were defined by the selection of breeder, coolant, structure, and neutron multiplier, if required, and by geometric characteristics of the design (Table III list materials considered by the BCSS). Of all the approximately 130 initial concepts (breeder/coolant/structure/neutron multiplier), the nine listed in Table IV were evaluated in detail.

TABLE II

DESIGN GUIDELINES FOR FUSION REACTORS IN BCSS[1]

	TOKAMAK	TMR
Reactor design basis	STARFIRE	MARS
Peak magnetic field (T)	10.0	5.0
Neutron wall load (MW/m^2)	5.0	5.0
First-wall heat flux (W/cm^2)	100.0	5.0
First-wall erosion (mm/yr)	1.0	0.1
Dose to TF coil (rad)	1.0E+10	1.0E+10

TABLE III

CANDIDATE FIRST-WALL/BLANKET MATERIALS[1]

BREEDING MATERIALS	COOLANTS	STRUCTURE	NEUTRON MULTIPLIERS
Liquid metals	H_2O	Austenitic steel	Beryllium
Lithium	Lithium	PCA	Lead
$_{17}Li_{83}Pb$	$_{17}Li_{83}Pb$	Manganese steel	
	Helium		
	Nitrate salt		
Ceramics		FS	
Li_2O		HT-9	
Li_8ZrO_6		Modified FS	
$LiAlO_2$			
Salt		Vanadium alloy	
Flibe		V-15 Cr-5 Ti	

TABLE IV

TOP RATED BLANKET CONCEPTS GIVEN FULL EVALUATION[1]

(Breeder/coolant/structure/neutron multiplier)

Li/Li/V	Li_2O/He/FS
Li/Li/FS	$LiAlO_2$He/FS/Be
LiPb/LiPb/V	$LiAlO_2$/H_2O/FS/Be
Li/He/FS	$LiAlO_2$/NS/FS/Be
Flibe/He/FS/Be	

Lithium was determined by the BCSS as the only viable breeding material for the deuterium-tritium fusion reactor. Solid compounds like Li_2O and $LiAlO_2$, liquid lithium, the $_{17}Li_{83}Pb$ eutectic alloy, and the flouride salt Flibe are the major breeder contenders for tritium breeding.

Solid Breeders

The leading candidates for the solid breeder concepts are Li_2O and several ternary lithium oxides, such as $LiAlO_2$ and Li_8ZrO_6. The Li_2O may provide adequate tritium breeding without the help of a neutron multiplier. Li_8ZrO_6 has a relatively high breeding potential and the possibility of better thermochemical stability compared to Li_2O. All other ternary ceramics considered require an effective neutron multiplier. $LiAlO_2$ was selected as the reference ternary solid breeder by the BCSS.

The principal issues associated with the use of solid breeding materials include:

1. fabrication/refabrication of the ceramic - two configurations were chosen for the solid breeder blankets: pressed and sintered plates and sphere-pac materials.

2. property data base - the items required to develop a data base included tritium solubility and diffusivity, surface desorption for tritium, thermal conductivity and expansion, and effects of radiation.

3. tritium recovery - tritium recovery imposes the greatest restriction on solid breeder operating limits. Tritium generated within the solid must diffuse to surface, desorb, and migrate to the helium purge where it will be removed.

Liquid Breeders

Lithium, $_{17}Li_{83}Pb$ eutectic alloy, and Flibe (47% LiF - 53% BeF_2) are the primary contendors for liquid breeder blankets. Disadvantages of lithium include its reactivity with water, air, and concrete. An advantage to using lithium is its solubility for tritium which will aid in tritium containment. Significant properties of LiPb include high density, reduced activity with air and water compared to lithium, and low tritium solubility resulting in high tritium pressures. Flibe is characterized by low thermal conductivity, relatively high melting point, and low tritium solubility.

Beryllium

Beryllium was chosen in the BCSS as the reference neutron multipliers for all $LiAlO_2$ and Flibe blankets. The primary concerns with beryllium are the resource limitation, irradiation swelling, tritium release, and salt compatability. Sufficient quantities of beryllium are available for the first and second generations of fusion reactor service. Recycling of beryllium will be required with special attention paid to recycle losses. Remote fabrication will be required due to induced radioactivity generated by the impurities in beryllium.

The generation of helium bubbles during irradiation will cause swelling. The volumetric swelling of beryllium can vary between 5 to 33% depending on the fluence and temperature history. Both inter- and intragranular helium bubble swelling will reduce the mechanical integrity of the beryllium. Beryllium used without containing structural material (as is the case for all Flibe and $LiAlO_2$ designs) may suffer loss of integrity resulting in coolant blockage, material relocation, and temperature hot spots. Safety concerns for specific blanket concepts involve tritium release and salt compatability of beryllium.

Design Concepts

Several concepts from BCSS utilizing beryllium as a neutron multiplier will be discussed. The concepts are based upon using

helium as a blanket coolant. Advantages to using helium include its chemical inertness, transparency to neutrons, no phase change, nonmagnetivity, nonconductivity, and the existence of systems for tritium recovery. The principal disadvantage is its low volumetric heat capacity leading to operating pressures in the range of 4 to 8 MPa. The pumping powers for the helium-cooled designs are of the order of 2 to 5% of the blanket thermal power.

A pressurized-module concept was selected for the reference design for all helium-cooled concepts in the BCSS. All the helium-cooled concepts are applicable to both the tokamak and TMRs. The first-wall for the TMR is simplified due to the absence of significant particle erosion or surface heat flux. An integral first wall is used for all the helium-cooled designs with the full flow of the inlet helium directed to the first wall. Whereas a simple channel is sufficient for the TMR, the first wall requires internal fins in the tokamak .

LiAlO$_2$/Be Design

The LiAlO$_2$/Be/HT-9 design concept[11] is applicable to both the tokamak and the TMR. Bare beryllium rods are placed in front of the LiAlO$_2$ to provide adequate neutron multiplication for tritium breeding. The LiAlO$_2$ is in plate geometry and clad in HT-9 to maximize the blanket breeder volume fraction. Tritium extraction is

accomplished by a helium purge stream with the help of added hydrogen for permeation control and for the control of potential surface tritium inventory.

For the TMR, the total blanket thickness, including the plenum, is 0.58 meters. In the tokamak, the total blanket thickness, including the plenum, is 0.41 meters for the inboard and 0.70 meters for the outboard locations (No beryllium is used in the inboard blanket to minimize the overall reactor dimension).[11]

FLIBE Design

In the helium-cooled Flibe blanket with beryllium multiplier[12] a 20-cm-thick bed of beryllium spheres, one centimeter in diameter, multiply neutrons while a concentrically adjacent region of silicon carbide (SiC) moderates the neutrons to maximize the production of tritium in the ^{6}Li within the molten flouride salt. The salt flows through tubes in the blanket and out to a separator where the tritium is removed. Helium flows radially outward through the beryllium pebble bed and SiC region providing heat transfer to the thermal conversion plant. The design can be converted into a fission-suppressed fissile breeder by doubling the beryllium zone and adding ThF_4 to the salt to produce approximately 6 tonnes of ^{233}U per year.[13]

B. <u>Summary of Evaluated Nuclear Data</u>

The $^9Be(n,2n)$ reaction proceeds by transitions through levels in ^9Be, ^8Be, ^6He, and ^5He.[14] The levels involved are wide and unstable with the end result of the reaction always being two neutrons and two alpha particles. In 1965, Perkins was the first to attempt to include details of this transition.[14] His evaluation was used in ENDF/B-III in the form of a single energy-dependent cross section with an angle-integrated secondary neutron spectra. In 1973, the format for ENDF/B was changed to allow the description of the reaction to include four time-sequential reactions. All of the ^9Be levels were assumed narrow, and the energy-angle correlation was neglected for the second neutron.[14] This format was used for ENDF/B-IV in 1974. An alternate procedure within ENDF/B formats allowed a doubly-differential reaction description in energy and angle, but this option was not used. In 1976 the doubly-differential beryllium neutron cross-section measurement by Drake et al.[14] was included in a pseudo-level representation of the (n,2n) reaction and a single-differential measurement by Hogue et al. was performed.[14] From these experiments, it was evident that the low-lying states in ^9Be were given too much importance in ENDF/B-IV. Beryllium was reevaluated using five levels in ^9Be. A request to include this in ENDF/B was not approved; hence the $^9Be(n,2n)$ reaction in ENDF/B-V is identical

to version IV. The evaluation; however, was included in Lawrence
Livermore National Laboratory's Evaluated Nuclear Data Library (ENDL)
which has no limitations on the numbers of levels or their respective
width.

C. Previous Integral Tests of Beryllium

To understand what has taken place in the area of integral
tests of beryllium, it is important to take a chronological look at
previous investigations. Studies of the neutron multiplication
properties of beryllium began in 1955 with Livermore Bulk Beryllium
Experiment.[15] In these experiments a cylindrical assembly of
beryllium, 8 inches in radius and 24 inches in height with a 14-MeV
neutron source placed in the center, was used to measure leakage
multiplication.

The assembly was constructed of rectangular bars of nuclear
grade (S-65) beryllium. A reentrant hole in the beryllium was
provided for the accelerator beam tube and an alpha counter was used
to monitor the neutron flux from the target. The target consisted of
a tungsten disk sputtered with titanium into which tritium was
absorbed. The assembly was placed into a 30 x 30 inch cylindrical
aluminum can. This can was supported by an adjustable table in an 8
foot high by 6.5 foot inner diameter aluminum tank containing a
$MnSO_4$ solution.

The experiment involved irradiation of the manganese bath with and without the beryllium present. Uniform activity samples were obtained by stirring the solution. The samples were measured to determine the ^{56}Mn activity decay corrected to the end of the irradiation. A correction was made for the relative neutron production in the target during the irradiation and a factor "p", the ratio of corrected counts to neutrons produced in the target during the bombardment, determined. The ratio of "p" values with and without beryllium in place determines the leakage multiplication. Several experiments were performed using two different baths. The resulting leakage multiplication obtained was 1.93 +/- 0.08 (95% confidence level).

Additional bulk beryllium experiments were performed in the 1970s by Cloth et al.[5] and Basu et al.[6] In these experiments, the neutron multiplication for varying thicknesses of beryllium was determined by measuring the neutron absorption in a thick polyethylene region which surrounded the beryllium. Measurements were performed using rectangular parallelpiped beryllium assemblies 8 cm, 12 cm, and 20 cm thick. The selection of a rectangular system was dictated by the physical form of beryllium available. In these measurements, the absorption rates in the polyethylene were determined using a BF_3 detector. The BF_3 count rates were normalized using dysprosium foils and wire activation measurements to determine the absolute neutron absorption rates.

The basis for this experiment was that the neutron multiplication could be determined by the ratio of the total number of neutron absorptions in an infinite media with and without beryllium in place.[6] The detection system was thought to provide neutron detection capabilities independent of space and neutron energy. However, the number of neutrons leaking out of the polyethelene region proved not to be negligible. Therefore, the measured multiplication was corrected for leakage from the polyethylene assembly by using MORSE Monte Carlo calculations.[16]

The measured neutron multiplication was also computationally corrected for neutron leakage from the central cavity that accommodated the target assembly and for the backscatter of neutrons into the beryllium from the polyethylene. These corrections were also obtained using MORSE. MORSE was also used to provide the computed multiplication for comparison with the corrected measured values. The MORSE calculations were performed using an isotropic point neutron source with cross sections from ENDF/B-III. The source strength for each experiment was normalized using ^{18}F activity of teflon foils around the DT source. Calculated leakage multiplication values obtained were 2.25 for the 20 centimeter beryllium 2.03 for the 12 centimeter beryllium and 1.79 for the 8 centimeter beryllium. Corresponding measured values were 1.62, 1.58, and 1.35 respectively, a difference of about 20-25% (Table V).

In 1983 Nargundkar et al.[17] performed a neutron

TABLE V

LEAKAGE MULTIPLICATION FOR DT NEUTRONS[5,6,9,14,17,19]

Experiment	4.6 cm	7 cm	7.9 cm	9.4 cm	12 cm	13.8 cm	19.9 cm
CALCULATED:							
Cloth					2.043		
Basu			1.79		2.03		2.25
Nargundkar *							1.54
Perkins(Basu)			1.705		1.901		
(Wong)	1.312						
Doyle (Basu)*			1.57		1.71		
(Cloth)*					2.13		
(LLNL Bulk)							2.19
Wong	1.132					1.64	1.89
MEASURED:							
LLNL Bulk							1.93
Cloth					1.725		
Basu			1.35		1.58		1.62
Nargundkar *							1.19
Wong	1.31					1.802	1.948

* - Values represent apparent multiplication only and are not
corrected for leakage out of the polyethylene or reflection from the
polyethylene back into the beryllium. These values are not directly
comparable with the leakage multiplication values listed in table.
        Values for Nargundkar are for BeO.

multiplication experiment in essentially the same geometry as previously mentioned using beryllium oxide instead of beryllium metal. Calculations were performed using MORSE-E [17] and the Los Alamos National Laboratory 30 group CLAW-IV cross section library and ENDF/B-III library of GAM-II structure both in P_3 scattering. The net leakage was the same for beryllium for both cross section sets; however, the neutron absorption and (n,2n) production differed significantly. For the polypropylene, the carbon absorption, the hydrogen absorption, and the net leakage differed significantly. This forced the experimenter to consider only the measured and calculated values for the apparent multiplication, the number of neutrons detected per source neutron, with no attempt being made to calculate the absolute value of neutron multiplication which is sensitive to carbon absorption and leakage from the assembly. Since the apparent multiplication was obtained as the ratio of hydrogen (or boron) absorptions with and without the beryllium multiplier, the different absolute values of carbon absorption and leakage from the two cross section libraries had no effect. The calculated value for apparent multiplication for the entire assembly was 1.54 while the measured value was 1.19 +/- 0.05.

Because of the stated discrepancies, Perkins et al.[14], in July 1984, used a Monte Carlo technique and doubly-differential measurements, to reevaluate the ^9Be(n,2n) reaction for future use in ENDF/B-VI. The general approach was to formulate a kinematics model

that described the various nuclear excitations levels and modes of breakup and then calculate doubly-differential cross sections which were then compared with available double-differential experimental data. The input to the model was varied, within the uncertainties of known nuclear structure information, until agreement between calculation and experiment was satisfactory. The evaluated data were tested, using the TART Monte Carlo Code by calculating appropriate parameters of integral experiments. The results of the analysis are shown in Table V. The results, even after reevaluation, still show a 20% discrepancy with the measured values from Basu's experiment;[6] however, good agreement was obtained for a 4.6 cm thick beryllium pulsed sphere measurement from Livermore.[14]

In February of 1984, Doyle and Lee[9], using the Tart Monte Carlo Code, recalculated and critiqued the multiplication values for the German[5], Indo-German[6], and Livermore Bulk Beryllium measurements.[15] For the Indo-German experiment the ratio of the measured leakage multiplication to Doyle's calculated leakage multiplication was 0.85 for 8 cm thick beryllium and 0.99 for the 12 cm thick beryllium. Doyle considered the agreement between the experimental and calculated values good considering the experimental uncertainties. The experimental uncertainties include: the change in neutron energy spectra at the detector locations which occur when the beryllium is removed (this could change the activation of the dysprosium foils because of a change in self-shielding) and localized

perturbations in the thermal flux caused by inserting the BF_3 counter or dysprosium foils.

Doyle performed the above calculations for pure and nuclear-grade beryllium.[18] His calculated values are listed with and without corrections for fast captures in carbon. The relative fraction of thermal and fast captures in polyethylene need to be accounted for to correctly represent 1/v absorptions.[9] To obtain his value for the apparent multiplication, he assumed nuclear grade beryllium, corrected for fast captures in polyethylene and integrated over the representative slab (the region in which measurements were actually taken)[6] instead of the entire polyethylene volume.

Doyle also modeled the LLNL Bulk beryllium experiment using the TART Monte Carlo Code. The nuclear beryllium modeled was the S-65 specification.[18] The target assembly and support structure in the tank were not included. The beam tube and alpha monitor tube were modeled as 0.3 cm thick aluminum tubes 1.25 inch in diameter. Two baths were used. The results of the calculated captures with and without beryllium present for the bath with 18.44 weight-percent $MnSO_4$ with a density of 1.25 gm/cm^3 are shown in Table V. The ratio of experimental to calculated values for manganese captures is 0.88 +/- 0.02.

Later in 1985, Wong et al. used the Pulse-Sphere Method[19] to measure neutron multiplication from hollow beryllium spheres of 4.6 cm, 13.8 cm, and 19.9 cm thicknesses (corresponding to 0.8, 2.42, and

3.5 mean-free-paths (MFP) for 14.8 MeV neutrons). The neutron leakage was measured by time-of-flight techniques at 7.28 meters with NE-213, Stilbene, and ^{6}Li glass scintillators. Measurements down to thermal energies were made using the ^{6}Li glass scintillator. The neutron flux was monitored by measuring the associated alpha particles with a surface barrier detector.

The efficiencies of the Stilbene and NE 213 detectors were determined by making pulsed-sphere measurements with a CH_2 sphere with the requirement that the calculated time-of-arrival spectra agree with the measured spectra. The efficiency curves obtained by doing this were absolutely normalized by comparing DT measurements with those obtained by a proton recoil counter whose efficiency was accurately known. The efficiency for the ^{6}Li glass detector was determined with an electron linac using a white neutron source with the detector 66 meters away and a small ^{235}U fission chamber of known mass at 7.2 meters.

Monte Carlo calculations were performed using the ALICE neutron transport code with the target assembly, source description and beryllium geometry modelled "exactly".[19] The ENDL-84 calculated leakage multiplication were 1.64 for the 13.8 cm assembly and 1.89 for the 19.9 cm assembly. The experimental leakage multiplication was reported as 1.802 +/- 0.02 for the 13.8 cm assembly and 1.948 +/- 0.02 for the 19.9 cm assembly (Table V). This gives a ratio of calculated to measured leakage of 0.91 and 0.97, respectively.

Chapter III   Experimental Apparatus and Procedures

A.   Spherical Shell Assemblies

Integral experiments were designed to directly measure the neutron leakage from spherical shells. Three polyethylene spheres were used to measure leakage from ^{252}Cf and DT neutrons (Table VI). The first polyethylene sphere (Poly-UT) had an internal cavity just large enough to accomodate the ^{252}Cf source. The second polyethylene sphere, also used with a ^{252}Cf source, was obtained from the Lawrence Livermore National Laboratory (Poly-LLNL). The third polyethylene shell was obtained from North Carolina State University (Poly-NCSU) and machined to accept the target assembly of the neutron generator.

Two sets of beryllium spheres were used (Table VI). The first set, on-loan from the University of Illinois (UI), consisted of two hemispherical shells of pure beryllium metal 7 cm thick (1.22 mean free paths (MFP) for DT neutrons) with a reentrant hole machined to accept the target assembly of the neutron generator. This set of shells also included a beryllium plug to seal the reentrant hole for measurements using point neutron sources.

The second set of beryllium shells was borrowed from Lawrence Livermore National Laboratory (LLNL). The set consists of numerous

26

TABLE VI

PROPERTIES OF SPHERICAL SHELLS

Sphere	Outer Radius (cm)	Inner Radius (cm)	Density (gm/cm^3)	Number Density (n/b-cm)	Shell Thickness (14 Mev) MFP	Shell Thickness (Cf) MFP
Poly-UT	22.86	0.25	0.934	0.08084 *	2.7	7.1
Poly-LLNL	25.5	16.5	.936	0.08038 *	1.1	2.8
Poly-NCSU	22.86	3.17	0.958	0.0822 *	2.3	6.2
Be-LLNL	12.6	8.0	1.85	0.1230	0.8	1.0
Be-UI	10.16	3.17	1.85	0.1230	1.22	1.6
Be-LLNL	27.94	20.06	1.85	0.1230	1.37	1.7
Be-LLNL/UI	12.6	3.17	1.85	0.1230	1.64	2.1
Be-LLNL **	21.84	8.0	1.85	0.1230	2.42	3.1
Be-LLNL **	27.94	8.0	1.85	0.1230	3.5	4.4

* - For hydrogen nuclei.

** - Hemispherical shells 12.6 cm $\leq$ r $\leq$ 20.1 cm missing.

hemispherical shells made of beryllium metal (Fig. 1). Shells 4.6 cm, 7.87 cm, 13.8 cm, and 19.9 cm thick, corresponding to 0.8 MFP, 1.37 MFP, 2.42 MFP and 3.5 MFP for DT neutrons, were used to provide data to compare with previous experiments.[19] The combination of this with the UI sphere provided a representative sample of mean free paths of interest for fusion reactor applications.[5,6,7,17,19,20] For thicknesses between $12.6 \leq r \leq 20.1$ cm only one-half of the hemispherical shells existed. The spheres were suspended on an aluminum stand (Fig. 2) with the source located 2.06 meters above the floor in the centroid of the room (Fig. 3) for all measurements.[21]

B. Neutron Sources

The neutron sources in the measurements consisted of a spontaneous fission source (^{252}Cf) and a neutron generator source of DT neutrons. These sources were chosen because they are well characterized and produce neutrons in the energy range of interest in beryllium studies.

The ^{252}Cf source (capsule type SR-CF-100) had dimensions of 9.4mm diameter and 37.6mm height with a cylindrical active source volume of 3.2mm x 3.2mm. The source was centered in the UI beryllium sphere using a styrofoam ball placed in the central void and suspended on the end of a target assembly for the LLNL spheres. The ^{252}Cf source was chosen because it has an energy spectrum that has been studied in great depth and is well characterized.[22]
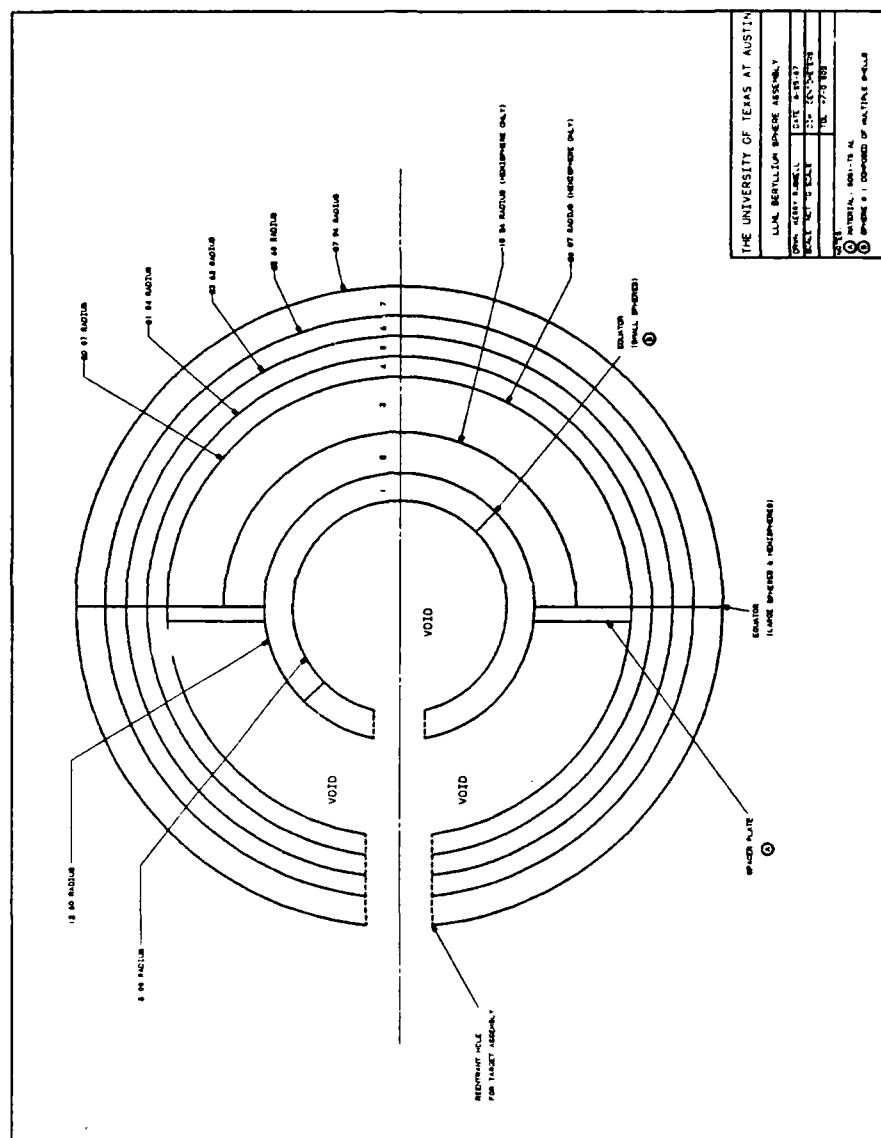
Fig. 1   The LLNL Beryllium Spherical Shell Assembly
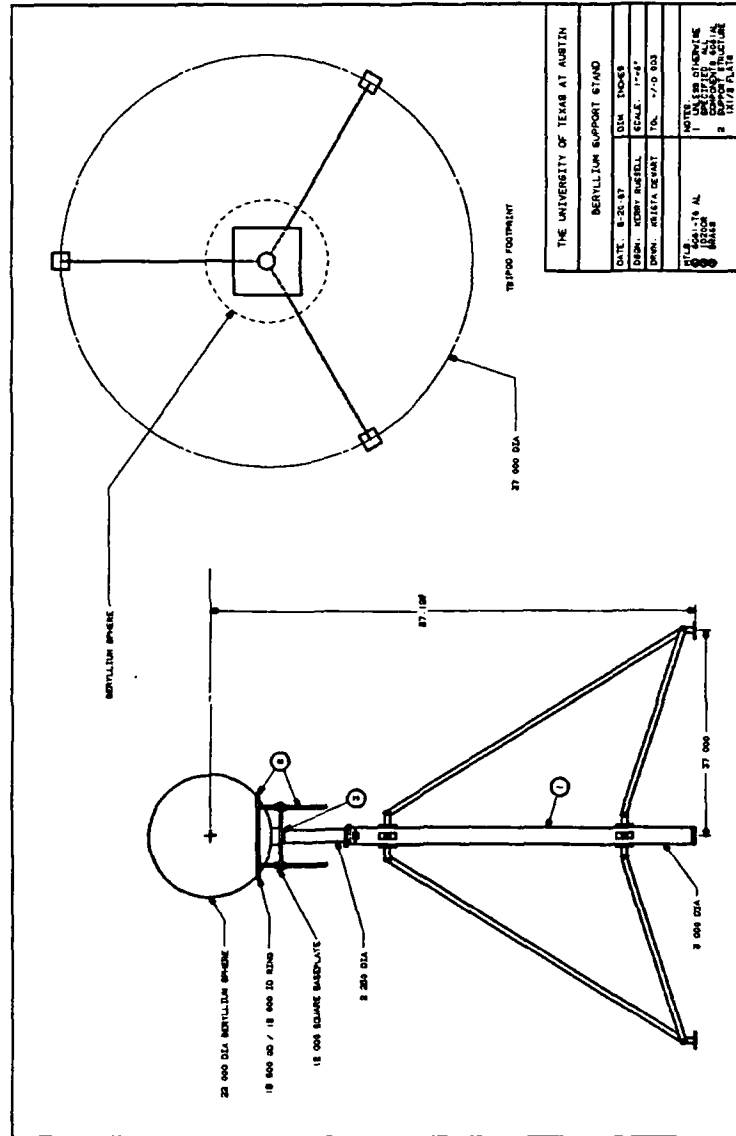
Fig. 2   The University of Texas Sphere Support Stand

31
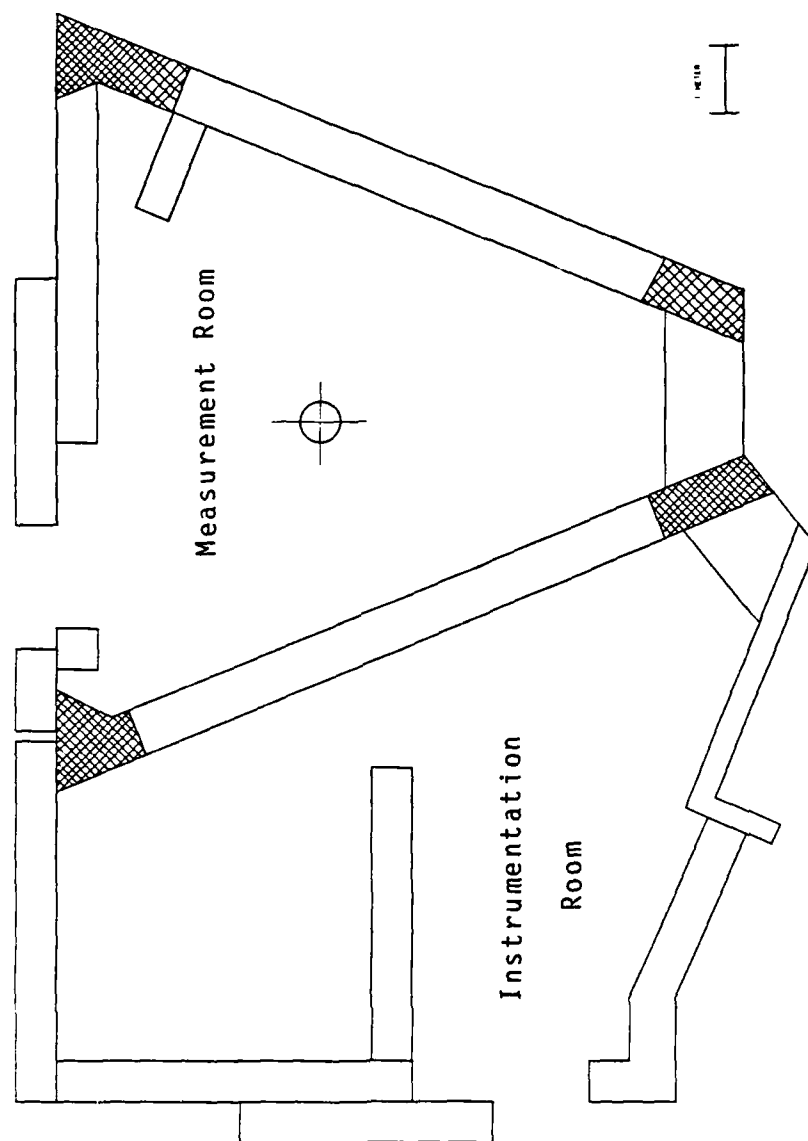
Fig. 3 Experimental Measurement Facility

The fusion neutron source used in this study

$$^2H + {}^3H = {}^4He + {}^1n + 17.8 \text{ MeV}$$

was generated with a Texas Nuclear Neutron Generator using a deuteron accelerating potential of 150 kV. DT neutrons were produced at a yield of approximately 10^8 n/sec/microamp of beam current. The DT neutrons are emitted isotropically in the center-of-mass system, but anisotropically in the laboratory system. The neutron flux distribution was measured in a relative manner using an NE-213 detector integrated above a 10 MeV bias (Fig. 4). The measurements were taken in the horizontal plane at a distance of 2 meters from the target. As can be seen the flux distribution is fairly isotropic especially along 0 and 45 degrees where the measurements were performed. The anisotropy seen around 135^0 is due to scattering of neutrons from the structural material supporting the target assembly and drift tube (Fig. 5). The angular distribution of the reaction products is assumed to be independent of the azimuthal angle.

Fluctuations in the deuteron beam current and tritium burnup in the target made it difficult to determine the DT neutron source strength using the beam current meter. Therefore, an associated particle detector was used to monitor both the neutron production rate
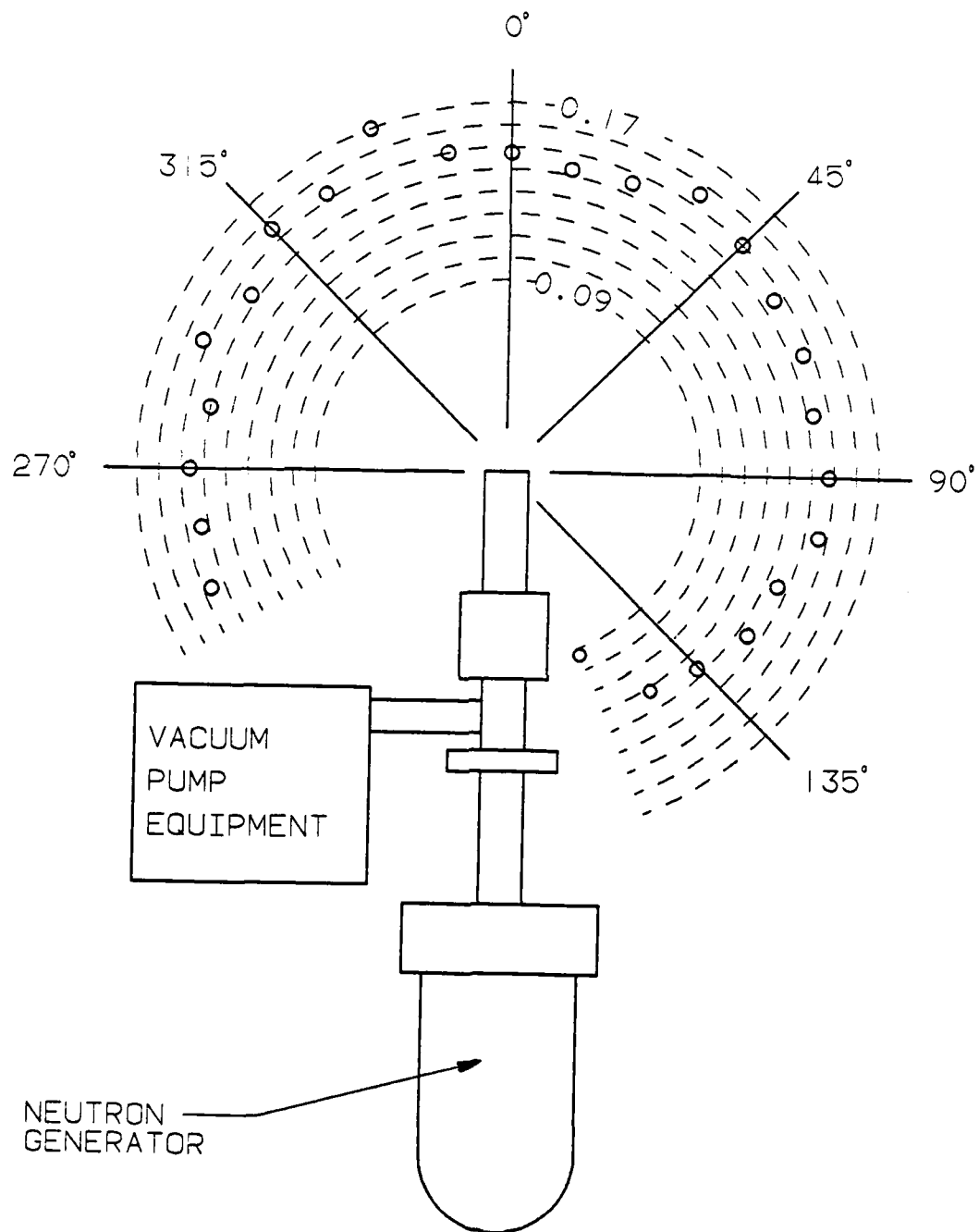
Fig. 4 Neutron Flux Distribution for DT Source
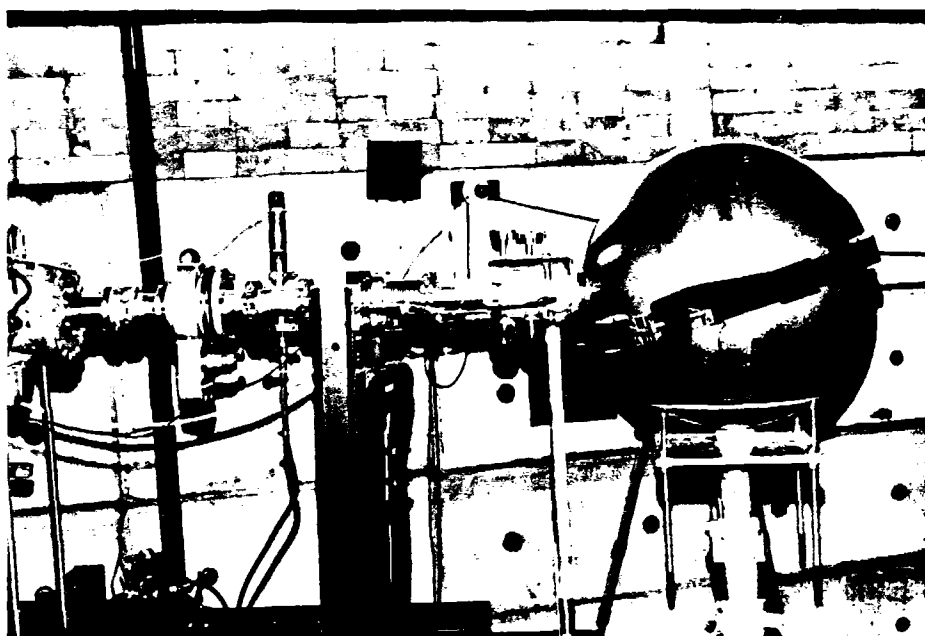
Fig. 5   Target Assembly with Support Stand

and the relative deuteron contamination rate by measuring the
associated particles with the DT and DD reactions.

C. Associated Particle System

The associated particle system was used to normalize the
neutron source strength between experiments. The associated particle
system is based upon measuring the charged particles emitted by the DT
and DD reactions to a defined recoil solid angle. The reactions of
interest are:

$$^{3}H(d,n)^{4}He \qquad E_n = 14.97 \text{ MeV} \qquad E_{alpha} = 2.79 \text{ MeV}$$

$$^{2}H(d,n)^{3}He \qquad E_n = 2.89 \text{ MeV} \qquad E_{3He} = 0.45 \text{ MeV}$$

$$^{2}H(d,p)^{3}H \qquad E_p = 2.62 \text{ MeV} \qquad E_{triton} = 0.61 \text{ MeV}.$$

The energy of the neutrons were calculated at 0° relative to the
incident deuteron beam while all other particles were measured at
175° relative to the incident beam where the associated particle
detector was located.

The associated particle system was housed in an aluminum
target assembly with the target electrically isolated from the

assembly by a Kelvex fitting (Fig. 5). A gate valve was used to separate the target assembly from the ion pump to allow quick target changes. A Tennelec surface barrier detector with a nominal active area of 50 mm^2 and depletion depth of 100 microns was mounted 46.5 cm from the target and operated at a bias of 74 volts. The angle of the detector (175° relative to the incident deuteron beam) was chosen to allow maximum clearance from the beam within the constraints of the target assembly (Fig. 6). The target assembly was designed with three sets of electrically insulated connections to which the electron suppression ring and two tantalum collimators with associated microamp meters could be attached (the current from the meters was used to align the beam since no view port existed in the assembly). The sides of the detector were surrounded with a heat shield to protect against boil-off electrons from the tantalum collimators while the front surface was covered with 0.1 mil thick mylar to protect the detector from elastically scattered deuterons. The beam spot was less than one centimeter in diameter so that no collimators were used.

A charged particle spectrum acquired with the associated particle system can be seen in Fig. 7. This spectrum was taken during a bare source measurement using a new target. By observing the associated spectrum, the molecular composition of the deuteron beam can also be estimated.[23] Alpha particles from DT reactions resulting from deuterons which constitute the D_2^+ beam component have a higher recoil energy into the backward direction (2.994 MeV)
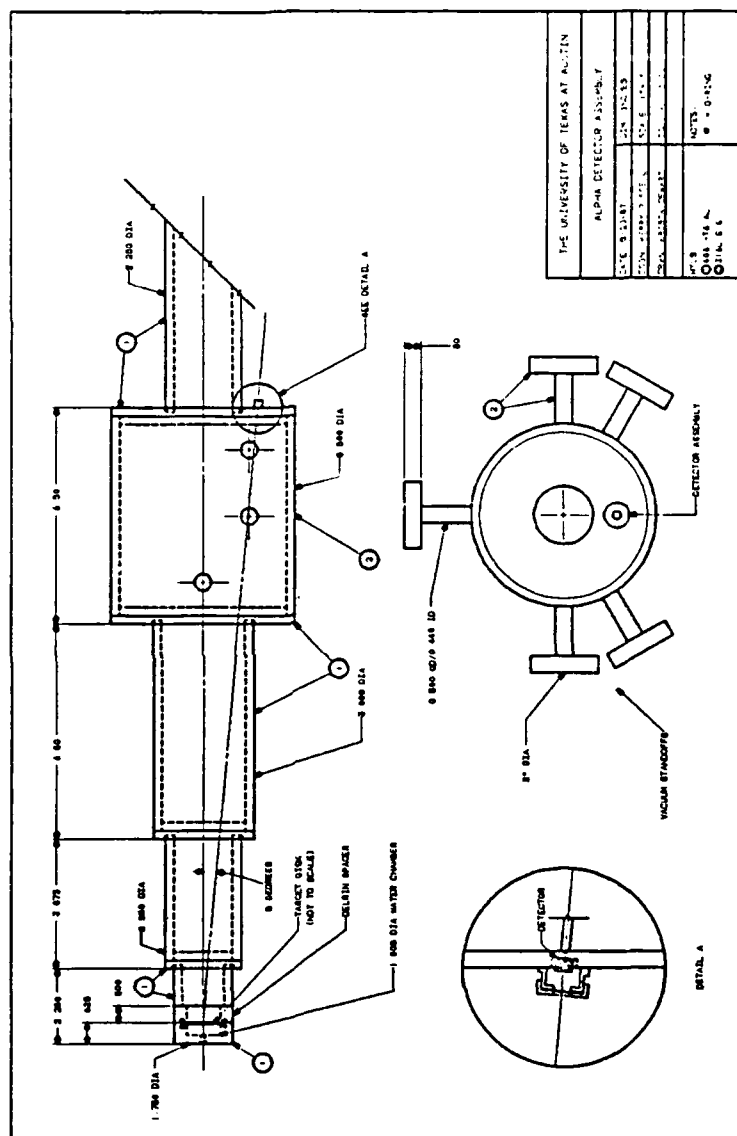
Fig. 6   The University of Texas Target Assembly
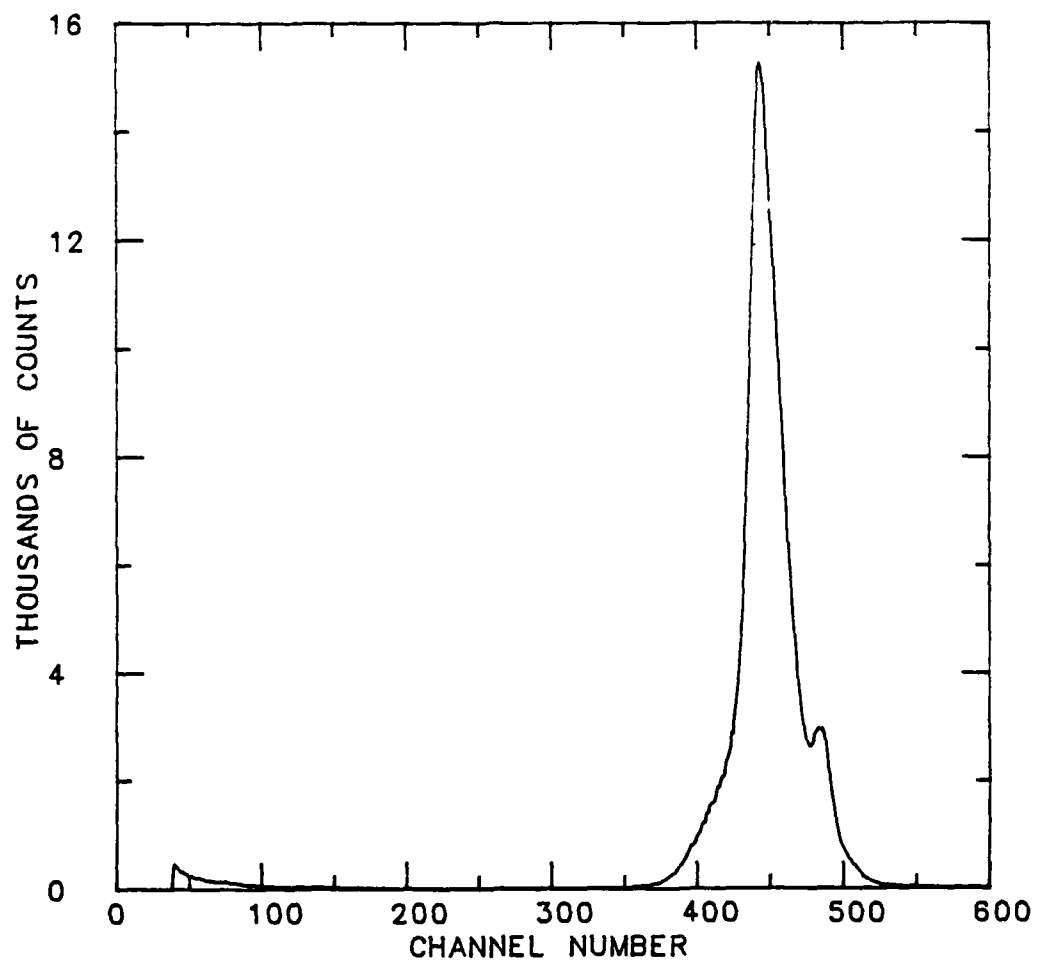
Fig. 7 Associated Particle Spectrum for New Target

than the recoiling alphas from the more energetic monatomic deuteron beam components (2.785 MeV).[23] The experiment described in Ref. 23 was performed with each new target to measure the beam composition (see Appendix B).

The associated particle system was also used to monitor neutrons produced by the $D(d,n)^3He$ reaction. These neutrons result from the interaction of incident deuterons with those embedded in the target. The resulting DD neutrons produce an undesirable component in the neutron spectrum.[4,24-27] Monitoring the rate of DD neutron production was accomplished by measuring the tritons emitted in the $D(d,p)T$ reaction. This is a competing reaction mode for the $D(d,n)^3He$ reaction, which produces tritons of sufficient energy to be observed above the noise in the associated particle system (Fig. 8). The triton peak was used to measure the DD contamination instead of the proton peak because the separation between the proton and alpha peaks was insufficient for accurate peak integration. The number of tritons detected can be related to DD neutron production using the ratio of the differential cross sections for the competing DD reactions.[24-27]

The burnup or depletion of the titanium tritide target was monitored using the triton-to-alpha count ratio in the associated particle spectrum.[25] With a new target, the triton peak is not observed (Fig. 7). As the target becomes depleted, the area of the triton peak relative to the alpha peak increases (Fig. 8). No targets
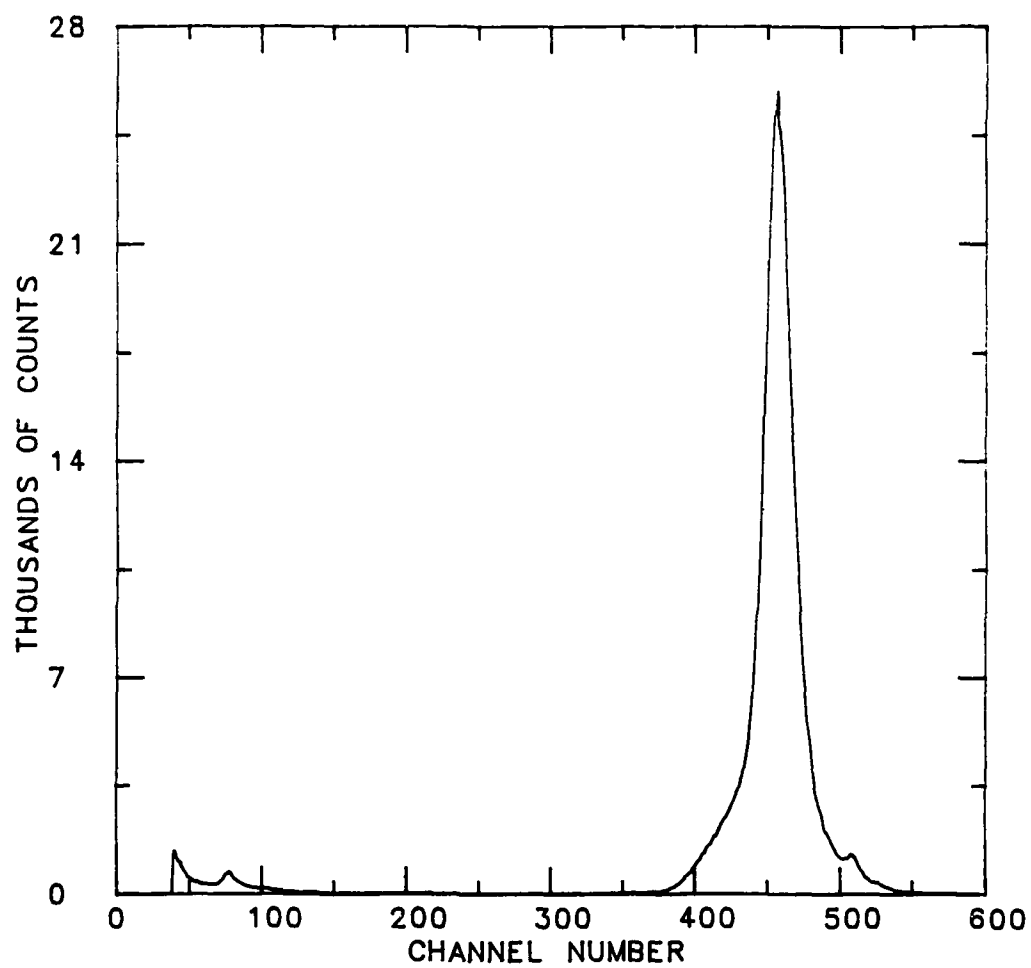
Fig 8. Associated Particle Spectrum for a Target

with 1 ma-hr Burnup

were used significantly past a burnup of 1 ma-hr, the point at which the contamination of the DT neutron spectrum by DD neutrons is reported to reach one percent.[28]

The stability of the associated particle system (i.e. the solid angle between the source and the detector and the efficiency of the surface barrier) was checked using two external neutron flux monitors (an NE-213 neutron detector and a Bonner sphere rate-meter). The ratio of neutrons detected versus the alphas detected was monitored for each experiment.

D. <u>NE-213 Spectrometry System</u>

An NE-213 spectrometry system was used to determine the relative DT neutron intensity as a function of the azimuthal angle by integrating proton recoil spectra above a 10 MeV bias. NE-213 liquid organic scintillators are well suited for neutron measurements in the presence of gamma background because their pulse shape characteristics allow identification and discrimination of neutron and gamma-ray induced events.[4,29]

Neutrons are detected by proton recoils in the NE-213 scintillator. The accumulated spectrum for a monoenergetic neutron is a distorted step function. Ideally, a rectangular proton recoil distribution up to a maximum proton energy equal to the incident neutron energy would result. The actual pulse-height distribution;

however, differs as a result of multiple scatters, escape of protons from the scintillator, neutron interaction with carbon, the nonlinearity of scintillator light output, and the operational characteristics of the photomultiplier tube.[4] In Fig. 9, a proton recoil pulse-height distributions for DT neutrons is shown. The rise at low pulse-heights is due to recoils from neutron scattering and interactions with carbon. The neutron flux was obtained by integrating the proton recoil spectra for pulse-heights above channel 60 in Fig. 9 roughly corresponding to 10 MeV neutrons. Measurements were performed at a distance of 2 meters from the target at 11.25 degree intervals in the horizontal plane as far around the neutron generator as possible. A plot of the results was shown previously can be seen in Fig. 4. The flux in the areas unaffected by structural material (neutron generator and pumps) appears somewhat isotropic implying that as an initial guess an isotropic flux distribution is valid for input into the transport codes.

E. Bonner Sphere Spectrometry System

The beryllium multiplication experiments were performed using a Bonner Sphere Spectrometer System.[30] The system was used to detect neutrons from known sources with and without beryllium interposed between the source and detector. The source-to-detector separation was sufficient to make backscatter corrections from the
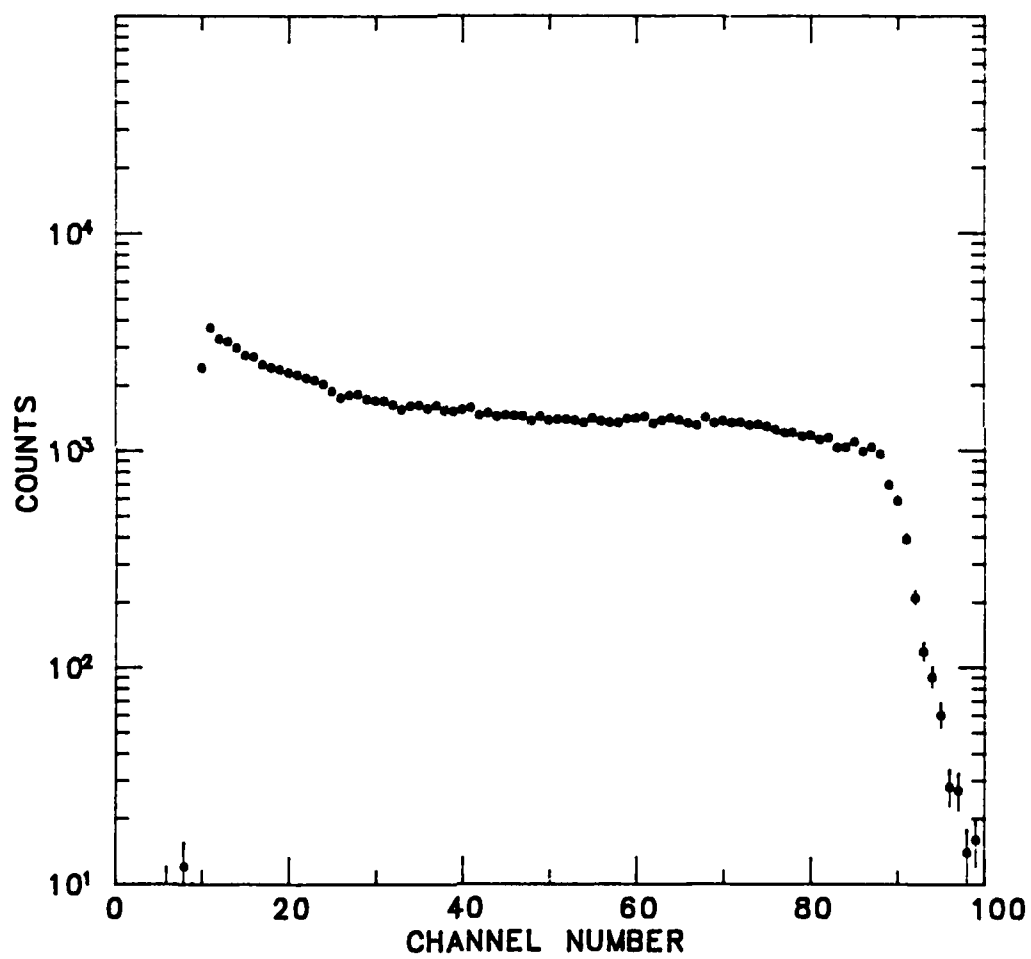
Fig. 9   NE-213 Proton Recoil Spectrum

detector to the source negligible.

The Bonner detector consists of a 4mm x 4mm diameter cylindrical ^{6}LiI(Eu) crystal-photomultiplier combination placed inside moderating polyethylene spheres (5.08 cm, 7.62 cm, 12.70 cm, 20.32 cm, 25.40 cm, 30.48 cm, and 45.72 cm diameter). Neutrons are detected by the reaction ^{6}Li(n,alpha)^{3}H which has a Q-value of 4.78 MeV. This large Q-value allows excellent discrimination against gamma-ray interactions in the crystal. Approximately 80% of the thermal neutrons incident on the crystal are absorbed in the first millimeter of the crystal so thermal neutron detection is essentially a surface effect, whereas the response to gamma-rays and high energy neutrons are proportional to the volume of the detector. By using a small crystal with a large surface-to-volume ratio, the proportion of counts not due to thermal neutrons is minimized.[30] Gamma-rays were subtracted using a linear background subtraction on a multichannel analyzer.

The response of each detector-sphere combination varies with energy. The discrete 171-group responses for each moderating sphere are plotted at the logarithmic midpoint of each neutron energy group in Fig. 10.[31] These responses were combined in a weighted Bonner sphere scheme to provide a relatively flat detector response for all energies of interest[32] and collapsed to form the response matrices used in the neutron unfolding code BUNKI[33]. See Table VII and Table VIII and Fig. 11 for the Bonner spheres and weights used and the
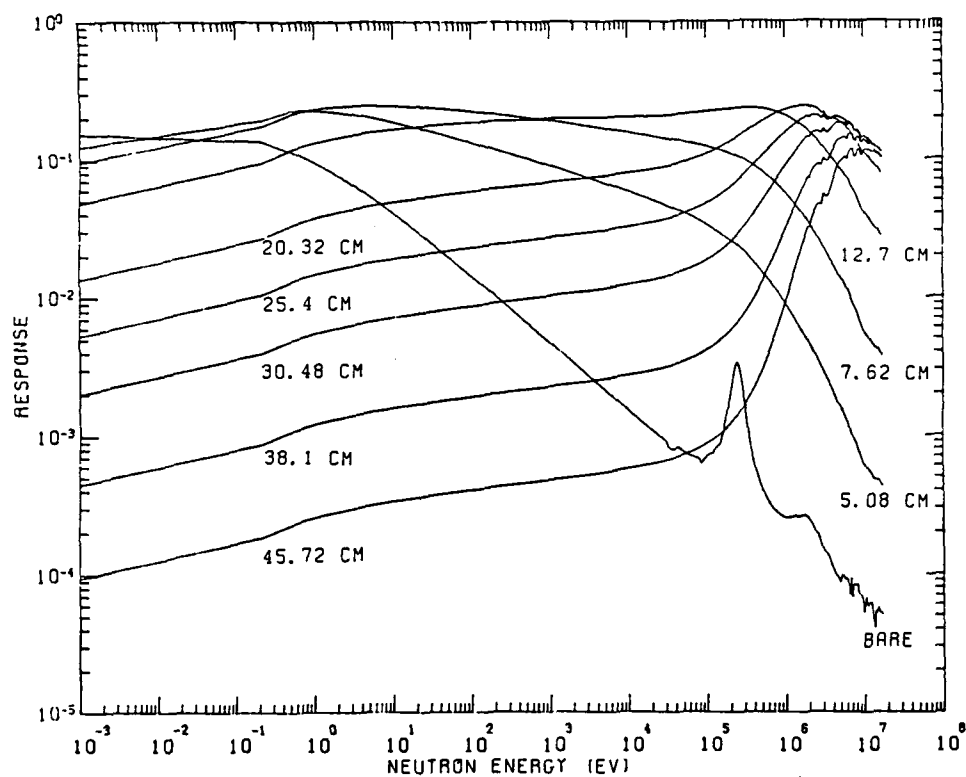
Fig. 10 The Calculated 171-group Responses

for the 5.08, 7.62, 12.7, 20.32, 25.4, 30.48, 38.1, and

45.72 cm diameter polyethylene spheres.

TABLE VII

BONNER SPHERE DETECTION COMBINATIONS AND THEIR WEIGHTS[*]
FOR DT NEUTRONS

Five-Sphere Combination

Bonner Sphere Diameter (cm)	Weighting Factor
7.62	2.745
12.70	1.604
20.32	3.368
25.40	-2.019
45.72	7.246

Three-Sphere Combinations

Bonner Sphere Diameter (cm)	Weighting Factor
12.70	5.293
20.32	-0.824
45.72	8.006

Bonner Sphere Diameter (cm)	Weighting Factor
12.70	5.008
25.40	-0.658
45.72	8.034

Bonner Sphere Diameter (cm)	Weighting Factor
12.70	4.903
30.48	-0.710
45.72	8.130

[*] - Calculated for UTA4.

TABLE VIII

BONNER SPHERE DETECTION COMBINATIONS AND THEIR WEIGHTS[*] FOR CF NEUTRONS

Four-Sphere Combinations

Bonner Sphere Diameter (cm)	Weighting Factor
5.08	-1.941
7.62	5.463
12.70	0.243
25.40	4.890

Bonner Sphere Diameter (cm)	Weighting Factor
5.08	-3.557
7.62	7.025
25.40	1.560
30.48	4.131

Three-Sphere Combination

Bonner Sphere Diameter (cm)	Weighting Factor
5.08	-4.164
7.62	7.562
30.48	5.923

* - Calculated for UTA4.
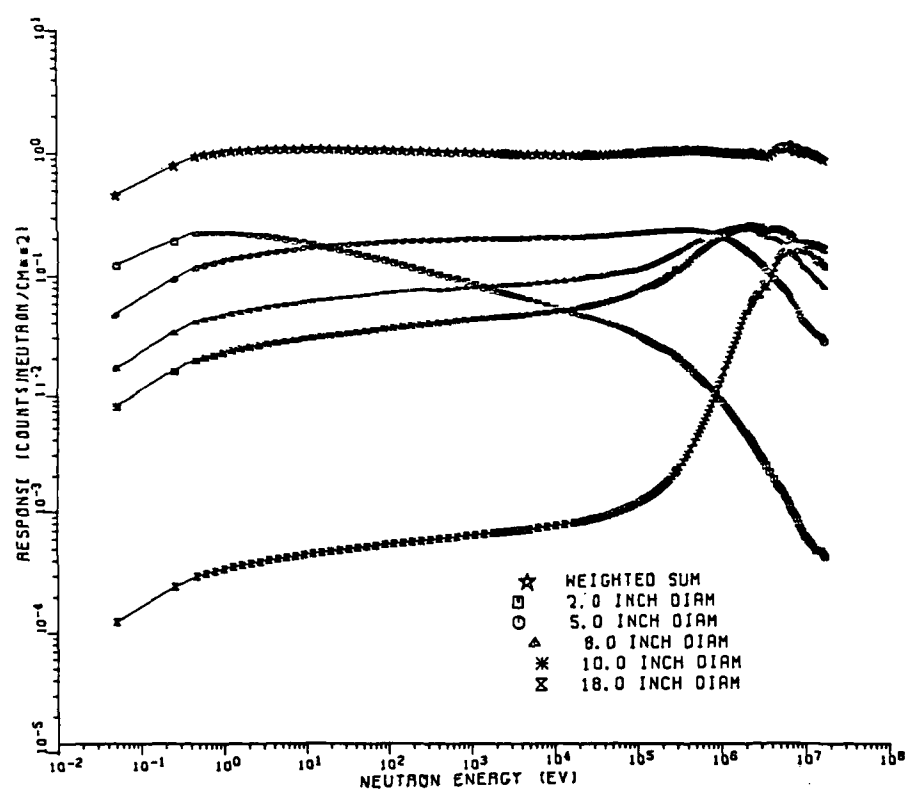
Fig. 11 Five Bonner Sphere Combination

resulting combined detector response.

F. Beryllium Multiplication Experiments

The beryllium multiplication experiments consisted of four
phases: 1) measurement of the count-rates with and without the
beryllium shells, 2) subtraction of the room-returned and
air-scattered contribution to the Bonner-sphere observed count-rates,
3) application of geometric correction factor to correct the
measurements from a distributed sources, and 4) determination of the
neutron leakage multiplication.

The physical layout of the measurement equipment and
measurement room used in this investigation was seen in Figs. 2 and
3. The floor was marked at its centroid and measurement locations at
specified angles.   Zero degrees corresponded to the direction of the
incident deuteron beam. Measurements at specified locations (between
1-2 meters from the source) were made by moving the detector along
designated angles (0° and 45°).

The basic model for room-return subtraction was that of
Hunt.[21]   He states that the count-rate times the
source-to-detector centerline distance squared results in a straight
line with the intercept containing information about the source
strength. Hunt refines this model with corrections for air- and
room-scattered neutrons and a finite detector geometry. Because in

this work, distributed sources were also measured with spherical
detectors another geometry correction factor was required.

Chapter IV Experimental Data Analyses and Results

A.   Analysis of Bonner Sphere Data

The beryllium leakage multiplication experiments were performed, using a Bonner Sphere Spectrometer System, to measure the neutron leakage produced by ^{252}Cf and DT neutron sources placed inside spherical beryllium shells. The room- and air-scattered corrected Bonner sphere count-rates and their associated error was input to the Bonner sphere unfolding code BUNKI[33] and used in a weighted Bonner sphere scheme[32] to obtain the leakage multiplication for each sphere. Leakage multiplication is defined as the number of neutrons leaking out of the beryllium sphere per source neutron introduced.

Room Return Corrections

Bonner sphere measurements require that the detector reading be corrected for all effects that may influence it i.e. neutron scattering by the floors, walls, ceiling, and air[21,34,35] to ensure that the count-rate observed is due to source neutrons alone. Numerous relationships have been proposed to fit measured Bonner sphere data.[21] A brief discussion of some of these procedures is

presented along with a detailed explanation of the linear fitting procedure chosen to subtract room-returned neutrons from the Bonner sphere counts.

For point sources and point detectors in large spherical measurement rooms the product of the detector count-rate $C(D)$ times the square of the distance between the source and the centerline of the detector D_0 should be a constant.[21,27,34,35,36] Deviations from this constant value are due to scattering of neutrons from the room and the air. Hunt[21] wrote the generalized functional relationship for the detector as a function of the source-detector separation distance as

$$(1) \qquad C(D) = K \ F_1(D) \ F_2(D) \ / \ (D + R_E)^2$$

where

$C(D)$ is the count-rate at a separation distance D_0 between the geometric centers of the detector and source,

D is the distance from the centerline of the source and the front edge of the moderating sphere,

$F_1(D)$ is a geometric correction factor that relates the detector response from a divergent beam to that obtained from a parallel beam (Corrects for departures from the inverse-square law),

$F_2(D)$ is the total air- and room-scattering correction factor,

R_E is the radius to the effective center of the detector which is taken to be synonomous in this case with the geometric center,[21]

i.e.

(2) $$D_0 = (D + R_E)$$

K is the source-detector characteristic constant which is

(3) $$K = B \, F_1(\theta) \, \varepsilon \, / \, 4\pi$$

where

$F_1(\theta)$ is the source anisotropy correction factor which corrects for the variation of neutron output with the angle of neutron emission relative to the axis of symmetry of the source,[35]

B   is the source strength,

ϵ is the detector efficiency.

For isotropic neutron sources at the center of large measurement rooms, the room-scattered component will be almost constant in a region near the source, while the air-scattered component will be inversely proportional to the separation distance.[21] Combining these "observations" allows $F_2(D)$ to be written as

$$(4) \qquad F_2(D) = 1 + A\,D_0 + S\,D_0^2$$

where

$A\ D_0$ is the air-scattered component. The air-scatter term although a function of D is written as a function of D_0 for simplicity without introducing significant error,

$S\ D_0^2$ is the room-scattered component.

The room-scattered component consists entirely of inscattered neutrons whereas the air-scattered component consists of both an inscatter component L and an outscatter component N so $F_2(D)$ can be written as

(5) $F_2(D) = 1 + (L - N)\ D_0 + S\ D_0^2$

where

N is the air linear attenuation coefficient obtain by weighting the neutron cross sections by the appropriate neutron energy spectrum.

Eqn. (1) with certain simplifying assumptions is the basis

for several models which have been shown to fit experimental data[21]. The shadow-cone technique[36], the polynomial fit model[21], and the Eisenhower, Schwartz, and Johnson (ESJ) or straight-line model[21,34] are three such models which were investigated for use in the present research.

The shadow-cone technique requires experimentally determining the air- and wall-inscattered components (L and S respectively) using shadow-cones placed between the detector and source to shield against direct source neutron interaction with the detector. With $F_1(D)$ approximately equal to one, Eqn. (1) can be written as

$$(6) \qquad \{[C(D) - S(D)] \; F_A(D)\}^{-1/2} = K^{-1/2} (D + R_E)$$

where

$\qquad$ $S(D)$ $\qquad$ is the inscattered count-rate,

$\qquad$ $F_A(D)$ $\qquad$ is the outscatter factor which is directly related to the average linear attenuation coefficient of air.

The experimentally obtained values for $C(D)$ and $S(D)$ are used with this equation to obtain the coefficient K using a weighted

least-squares technique. The shadow-shield technique has been proven to be the best of the three for determining the free field fluence.[21,37] However, due to the physical size of the shadow shields necessary to shadow the Bonner spheres from the beryllium spheres, this method could not be used.

The polynomial fit utilizes Eqn. (4) and Eqn. (1) to give

$$(7) \qquad C(D) \, D_0{}^2 \, / \, F_1(D) \;=\; K \, \{1 + AD_0 + SD_0{}^2\}.$$

Measurements of the count-rate data, $C(D)$, corrected by $F_1(D)$, are used to obtain the coefficients K, A, and S using a weighted least-squares fit.

The polynomial fit model does not work well in small to medium sized measurement rooms such as the one used here.[21,37] In fact the polynomial fit has been described as "just that - a two parameter fit to the data where the physical significance of the parameters may not be obvious."[35,38] Because of this and the small, irregular size of the measurement facility, the polynomial fit was not chosen.

The Eisenhower, Schwartz, and Johnson model[21,34] is based upon using Eqn. (1) and (4) while utilizing the fact that the air-scatter component is small relative to the room-returned contribution so that $F_2(D)$ can be written as

$$(8) \qquad F_2(D) = (1 + S \, D_0{}^2) \, (1 + A \, D_0).$$

Eqn. (1) becomes

$$(9) \qquad C(D) \, D_0{}^2 \, / \, [F_1(D) \, (1 + A \, D_0)] = K(1 + S \, D_0{}^2).$$

The count-rate data as a function of the separation distance corrected by $F_1(D)$ and an air-scatter correction is fit with this equation utilizing a weighted least-squares approach to obtain the characteristic constant K and the room-scattered component S.

Use of this method requires the values of the air scattered coefficient A to be known. Values for A were obtained using Monte Carlo calculations by Eisenhauer et al.[34] for bare ^{252}Cf ($<E> = 2.0$ MeV), ^{252}Cf moderated by D_2O ($<E> = 0.5$ MeV), and AmBe sources ($<E> = 4.5$ MeV). These values were based upon an air composition of nitrogen and oxygen with 50 percent relative humidity, temperature at $21^{o}C$, and pressure of 10^5Pa. The values obtained for the 22.86 cm and 7.62 cm diameter spherical remmeter were extrapolated to other sphere diameters by Hunt.[21] The values for A from the bare ^{252}Cf were used for bare ^{252}Cf spectra and spectra from ^{252}Cf inside the beryllium spheres. The AmBe values were the only ones in the literature for medium to high energy neutrons; therefore, were used for all DT measurements.

More accurate air-scattered values were obtained by Eisenhauer et al. utilizing the Monte Carlo Code MCNP.[39] The

values for A were obtained for each Bonner sphere for The University
of Texas Bonner Sphere Response Matrix (UTA4)[31]. This was
accomplished by collapsing the 171 group response matrix into 20
groups with compatible energy ranges as listed in Ref. 39,

i.e.

$$\text{(10)} \quad R_i' = \sum_{n=1}^{171} \Delta E_n R_n/(E_{i+1}-E_i) \qquad i = 1,2,\ldots 20.$$

The collapsed response matrix for each energy group was used
to weight the total neutron fluence (free-field neutron fluence plus
the net neutron fluence due to air-scatter) to obtain the response per
unit fluence, σ, to the spectrum in air at 5 meters, i.e.

$$\text{(11)} \quad \sigma = 4 \pi r^2 \sum_{i=1}^{20} R_i' \phi_t^i/\phi_t$$

where

$$\phi_t = \sum_{i=1}^{20} \phi_t^i$$

$$\text{(12)} \quad \sigma_0 = 4 \pi r^2 \sum_{i=1}^{20} R_i' \phi_0^i/\phi_0$$

where

$$\phi_0 = \sum_{i=1}^{20} \phi^i_0$$

is used to weight the free-field fluence to obtain the corresponding response σ_0 to the source spectrum.

The relative response per meter due to air-scatter is obtained from the product of σ/σ_0 times $\phi t/\phi_0$ at 5 meters as follows:

$$(13) \qquad R_s/R_0|_{1m} = [(\sigma/\sigma_0 \quad \phi t/\phi_0)_{5m} - 1] / 5.$$

The new values of the relative response or A values are shown in the last column of Table IX along with the values of A used in this investigation. The values of A from Eisenhauer et al.[39] are higher by about 40% compared to the values used in the present research. A study of the effects of varying A on the final beryllium leakage multiplication; however, showed that variations in A by a factor of 10 affected the multiplication by less than one-half percent (Appendix D). Therefore, the value for A selected need not be exact and does not warrant a large computing effort to determine. Therefore the values listed in Ref. 21 were used with an uncertainty of 50%.

TABLE IX

AIR SCATTER COEFFICIENTS

Bonner Sphere Diameter (cm)	* (21) AmBe	(38) AmBe	^{252}Cf (21)	^{252}Cf (38)
Bare	.014	....	.017	.0256
5.08	.014	....	.017	.0254
7.62	.014	.016	.017	.02164
12.70	.01	....	.012	.01745
20.32	.008	....	.01	.01366
25.40	.008 **	.009 **	.01 **	.01171
30.48	.008	....	.01	.01002
45.72	.008	....	.01	.006

* - Calculated from values given in Reference 21.

**- Actually a 22.86-cm diameter moderating sphere.

Geometric Correction Factor

The geometric correction factor $F_1(D)$ was originally derived by Axton[40] for spherical detectors in an isotropic radiation field and later for a spherical source and point detector by Ing and Cross.[41] This factor allows for partial-illumination of the detector at very short distances resulting in deviations from the inverse square law.[21]

The correction factor was obtained by determining the difference in neutrons detected by a spherical detector from a point source versus a spherical detector from a parallel beam upon which the detector response was calculated. In particular, the excess neutrons observed N, is equal to the total number of neutrons per second S striking the sphere (of radius r) from a point source (located a distance d from the center of the sphere which produces a unit flux density at the position of the center of the sphere in the absence of the sphere) minus the total number P striking the same sphere in a parallel beam of unit flux density relative to the number P,

i.e.

(14) $$N = (S - P) / P$$

where

$$S = 2\pi d^2 [1 - (1 - r^2/d^2)^{1/2}]$$

or the current on the surface of the sphere from a diverging neutron flux of 1 n/cm^2 at the center of the sphere

$$P = \pi r^2$$

or the current on the surface of the sphere from non-divergent neutron field such that

$$(15) \qquad N = \{ 2d^2/r^2 \} [1 - (1 - r^2/d^2)^{1/2}] - 1$$

and the geometric correction factor $F_1(D)$ for a point source (PS) and spherical detector is written as

$$(16) \qquad F_1^{PS}(D) = 1 + \delta N$$

or,

$$(17) \quad F_1^{PS}(D) = 1 + \delta \{ 2d^2/r^2 [1 - (1 - r^2/d^2)^{1/2}] - 1 \}.$$

The expression indicates the response of the detector is increased above that expected solely from the inverse square law. The parameter δ accounts for the relative effectiveness of the excess neutrons in producing a count in the detector. The value of $\delta = 2/3$ has been suggested as being generally applicable[21] and was adopted in this investigation. Values for $F_1^{PS}(D)$ are listed in Table X.

The point-source geometric correction factor was used to correct the count-rate data obtained from the bare source measurements (^{252}Cf and DT). One reference indicated a different correction factor may be required when measuring a spherical distributed source with a spherical detector.[35] Eisenhauer et al.[35] suggested a correction factor containing a product of two factors of the type shown in Eqn. (15) using the source radius in one factor and the detector radius in the other; however, the lack of experimental data at that time precluded a definitive formulation.[35]

The search for the appropriate factor lead to radiative shape factors used in heat transfer. Radiation shape factors between two spheres have been numerically evaluated and plotted for various sphere sizes and separation distances.[42,43,44] An analytical expression was compared to these numerical evaluations by Felske and found to be accurate to within 1-1/2% over the parameter range of interest in this investigation.[45] The shape factor between two spheres of finite size and spacing is known to be greater than the shape factor calculated by replacing one by a point source.[43,44,45] The point

TABLE X

GEOMETRIC CORRECTION FACTORS

Bonner Sphere Diameter (cm)	D(cm)	PS $F_1(D)$	DS * $F_1(D)$
5.08	100.	1.0001	1.0137
5.08	200.	1.0000	1.0033
7.62	100.	1.0002	1.0138
7.62	200.	1.0000	1.0032
12.70	100.	1.0007	1.0142
12.70	200.	1.0001	1.0034
20.32	100.	1.0017	1.0153
20.32	200.	1.0004	1.0037
25.4	100.	1.0027	1.0163
25.4	200.	1.0007	1.0040
30.48	100.	1.0039	1.0175
30.48	200.	1.0010	1.0043
45.72	100.	1.0089	1.0227
45.72	200.	1.0022	1.0055

* - For R = 27.94 cm sample sphere.

source shape factor was modified to account for the finite size of the radiating sphere by assuming the kernel of the double area integration was separable.[45]

Rewriting Eqn. (17) in terms of shape factors:

$$(18) \qquad F_1^{PS}(D) = 1 + \delta[\{4d^2/r^2\} (F_{12}^{PS}) - 1]$$

where

$$F_{12}^{PS} = \text{point source shape factor,}$$

$$F_{12}^{PS} = [1 - (1 - r^2/d^2)^{1/2}] / 2.$$

The point source shape factor is replaced by the distributed source shape factor obtained from Felske[45],

$$(19) \quad F_{12}^{DS} = [1-(1-r^2/d^2)^{1/2}][1-(1-R^2/d^2)^{1/2}](d/R)^2$$

so the geometric correction factor for the distributed source (DS) can be written as

$$(20) \qquad F_1^{DS}(D) = 1 + \delta N$$

where

$$N=\{[1-(1-r^2/d^2)^{1/2}][1-(1-R^2/d^2)^{1/2}]$$
$$[d^2/R^2]4d^2/r^2\}-1.$$

Values for $F_1^{DS}(D)$ can also be seen in Table X. This new geometric correction factor was experimentally verified using Eqn. (1) to fit data obtained from a calibrated ^{252}Cf placed inside a 45.72 cm diameter polyethelene sphere. The measured data was compared to one-dimensional calculations obtained by ANISN. The results are shown in Table XI.

Propagation of Errors

In this investigation, the errors in the source strength K are used only on a relative basis as weighting factors in the BUNKI unfolding code.[33] The errors generated by BUNKI for the neutron fluence are obtained from the difference between input data and the final generated fit, weighted by the importance of that particular sphere data by the inverse of the relative variance. To provide this input variance, standard error propagation procedures were followed.[46]

TABLE XI

VERIFICATION OF THE DISTRIBUTED SOURCE
CORRECTION FACTOR

UT-Polyethylene for ^{252}Cf neutrons:

    ANISN: 0.0548

    Measured multiplication (point source)   = 0.058(.003)

    Measured multiplication (distributed source) = 0.055(.003)

Numbers in parentheses represent one standard deviation in the
measurement uncertainty.

When dealing with the ESJ model, the dependent variable is written as

(21) $$y = C(D) [D_0]^2 / (1 + A D_0) F_1(D)$$

with

$$y = f[C(D), D_0, A, r, R]$$

where

$C(D)$ = count-rate at distance D,

D_0 = center-to-center distance between source and detector,

A = air scatter term,

r = radius of Bonner sphere,

R = radius of beryllium sphere.

The error in the ordinate then can be written as

$$(22) \qquad \sigma_y = \{[\sigma_{C(D)}]^2 (\partial y / \partial C(D))^2 + [\sigma_{D_o}]^2 (\partial y / \partial D_o)^2$$
$$+ \quad [\sigma_A]^2 (\partial y / \partial A)^2 + [\sigma_r]^2 (\partial y / \partial r)^2$$
$$+ \quad [\sigma_R]^2 (\partial y / \partial R)^2 \}.$$

Since both the Bonner and beryllium spheres were machined to precise tolerances σ_r and σ_R were negligible relative to the other errors. The error in specifying A was set equal to 50% to account for the differences in A determined by Hunt[21] and Eisenhauer et al.[39] σ_{D_o} was set at 3mm. The variance in the count-rate data included error propagated for background subtraction of gamma-rays under the alpha peak and normal Poisson statistics in the counting data.

The independent variable of the linear model is simply $[D_o]^2$ so that

$$(23) \qquad \sigma_{[D_o]^2} = 2 \, \sigma_{D_o} \, D_o.$$

Normally the error in the independent variable is ignored when its magnitude is small relative to the error in the dependent variable. In the case of some of the measurements with a low neutron emission rate, as was the case when using the normalized count data from the

neutron generator, the errors in the independent variable were sometimes larger than the errors in the dependent variable. Therefore, errors were allowed in both axes. The general relation for this, assuming the errors in the independent and dependent are uncorrelated, is

$$(24) \qquad \sigma_i = \{C_1 [\sigma_{yi}]^2 + C_2 [\sigma_{xi}]^2\}^{1/2}.$$

This equation served as the basis for the weighted least-squares program chosen to fit the data.[47] After each fit, the results were subjected to tests to ensure the goodness of fit obtained. The errors in the coefficients were used with the "t"-distribution to determine the confidence interval for the coefficients

$$(25) \qquad a_k - S_{ak} * t(n-p) < A_k < a_k + S_{ak} * t(n-p)$$

where

$n-p$ = the number degrees of freedom,

A_k = the true coefficient,

a_k = the computed coefficient,

S_{ak} = error computed for the coefficient.

The "t"-distribution approaches the normal distribution as the number of degrees of freedom approach infinity. In most cases at least ten data points were obtained for each sphere so that the value for "t" was approximately 2.3 (the 95% confidence level was chosen to represent the data).

Response Matrix Generation

All analysis techniques using Bonner spheres require a knowledge of the detector response. Originally, three energy-dependent response matrices were available for use at The University of Texas.[30,31,49] Bramblett[30] published the original work on the Bonner sphere spectrometer with an experimentally determined response for thermal neutrons and neutrons of energy 0.05 to 15.1 MeV. Responses were then estimated for neutrons of energy between .025 eV and 50 keV since no neutron sources in this energy range existed. This response was called M60. Hansen and Sandmeier[50] using the adjoint transport technique calculated the response for a set of Bonner spheres. These responses plus those of

moderators of diameters 25.40 cm, 40.64 cm, 45.72 cm, and 50.80 cm were reported by O'Brien et al.[51] for energies extending to 160 MeV (referred to as M65). In 1973, Sanna[49] calculated a 31 bin response matrix for 4mm x 4mm ^{6}LiI(Eu) detector for neutron energies between thermal and 400 MeV using the adjoint method of Hansen and Sandmeir. This response matrix is called SAN4.[52]

In 1983, new response matrices were calculated using ANISN at The University of Texas[31] using ENDF/B-IV[53] and a fine group structure (171 groups). The approach used was similar to the one employed by Sanna[49] using the adjoint transport technique of Hansen and Sandmeier.[50] The adjoint current at the moderating sphere surface was calculated using the macroscopic ^{6}Li(n,alpha) and ^{7}Li(n',n'alpha) cross sections as the adjoint source which was distributed in the detector volume at the center of the moderating sphere.

To perform a one-dimensional calculation, the cylindrical detector used in the Ludlum spectrometer was replaced with an equivalent spherical detector. Sanna used a sphere radius with a set of adjusted ^{6}Li cross sections that forced the collision probability for the equivalent sphere to be equal to that of an infinite cylindrical detector of the same radius for each neutron energy group. Sanna calculated the collision probabilities using the results of Case, DeHoffman, and Placzek[54] for spheres and infinite

cylinders and then adjusted the cross sections. In The University of Texas calculations, the 4mm x 4mm cylindrical LiI(Eu) detector was replaced by a spherical detector having the same surface area. The adjoint source was generated using the sum of the macroscopic ^{6}Li(n,alpha) and ^{7}Li(n,n' alpha) cross sections. These cross sections were adjusted with weights determined by matching the collision probabilities for a finite cylinder[55] rather than for an infinite cylinder. The responses for the bare detector and the 5.08 cm, 7.62 cm, 12.70 cm, 20.32 cm, 25.40 cm, 30.48 cm, and 45.72 cm moderating spheres were calculated. Addition refinements included the aluminum encapsulation of the detector and calculations for the cadmium covers for the bare detector, the 5.04 cm, 7.62 cm, 12.70 cm diameter Bonner spheres.

Calibration of Bonner Sphere Response Matrices

Since the previously mentioned calculated responses for the 4mm x 4mm LiI detector of Sanna[49](SAN4)[52] and Davidson and Hertel[31] (UTA4)[52] assumed a detector efficiency of 1.0, they should be experimentally normalized.[56] To accomplish this, a calibrated ^{252}Cf source was used. The flux of this well-known spectrum (22,52,56) was folded with the calculated Bonner sphere

response and compared to the experimentally observed count-rate, obtained using the shadow-shield method[21], for each Bonner sphere.[37] The ratio of these counts for each sphere represents the calibration factor for each sphere for the response matrix of interest. (See Table XII for the calibration factors.)

Spectrum Unfolding

Unfolding neutron spectra using Bonner spheres involved solving an equation of the form:

$$(26) \qquad Y_j = \int_{Emin}^{Emax} A_j(E) \; X(E) \; dE \qquad j = 1,2,\ldots.M$$

where

$X(E)$ = neutron fluence distribution of energy "E",

Y_j = response of the jth detector,

$A_j(E)$ = response of the jth detector to neutrons of energy E,

M = total number of Bonner spheres.

TABLE XII

CF_j VALUES BASED ON ^{252}Cf USING THE SHADOW SHIELD MODEL[36]

Bonner Sphere Diameter (cm)	Texas Response Matrix	Sanna Response Matrix (HASL-267)
5.08	1.18 +/- 0.04	0.654 +/- 0.004
7.62	1.09 +/- 0.03	0.691 +/- 0.003
12.70	1.05 +/- 0.03	0.757 +/- 0.003
20.32	1.05 +/- 0.03	0.818 +/- 0.003
25.40	1.02 +/- 0.03	0.820 +/- 0.003
30.48	1.00 +/- 0.03	0.814 +/- 0.003
45.72	1.09 +/- 0.04	0.876 +/- 0.003

Eqn. (26) is a degenerative case of the Fredholm integral equation of the first kind which can be solved exactly, only if $A_j(E)$ is an integrable analytical function. Since this is not the case for Bonner spheres, Eqn. (26) must be replaced by a system of linear equations by dividing the energy region into several regions having constant detector responses and fluences, i.e.

$$(27) \qquad Y_j = \sum_{k=1}^{N} A_{jk} X_k \qquad j=1,2,\ldots M$$

where

Y_j = response of the jth detector,

A_{jk} = response of the jth detector to neutrons in the kth energy interval,

X_k = neutron fluence in the kth energy interval,

N = total number of energy intervals.

Eqn. (27) can be written in matrix form as:

$$(28) \qquad \underline{Y} = A\underline{X}$$

where N, the number of energy intervals, usually is greater than M, the number of Bonner spheres, so no unique solution exists.

Methods for solving the above equations for neutron spectrometry have been summarized by Nachtigall and Burger.[57] One method which finds a non-negative solution by minimizing, through an iterative recursion procedure, the deviation between the measured and calculated detector response.[58] This method was modified by O'Brien et al.[51] and Sanna[59], who called the computer code BON31G. Doroshenko et al.[60] have described another iterative recursion method for spectrum unfolding. Brackenbush and Scherpelz[61] wrote a code, SPUNIT, which uses this algorithm.

Both of the above methods have been incorporated into the unfolding code, BUNKI by Johnson.[33] A version written for the IBM-PC, with plotting capability, calculates particle fluence as a function of energy or total fluence using either the BON31G or the SPUNIT algorithms. The initial spectrum may be specified by the user or a Maxwellian initial spectrum may by determined by using MAXIET, an algorithm originally devised for use in the neutron unfolding code YOGI.[33] In this investigation the use of SPUNIT was chosen based upon the recommendation of T.L. Johnson of the Naval Research Laboratory.[38]

The response matrices used in this investigation were limited to SAN4 and UTA4 because they "consistently provide reasonably shaped

spectra that fit the sphere data within experimental error, and agree well with other calculated and experimental data".[52] The average energy computed for spectra unfolded using UTA4 tends to be lower than SAN4. According to Johnson the fluence does not vary more than 15% with the choice of matrix.[52] Upon further analyses however, the combination of UTA4 with its calibration factors seemed to provide more consistent results and was chosen as the response matrix for all data analyses (Appendix C). The choice of this response matrix and the unfolding algorithm SPUNIT in the program BUNKI were deemed to provide the best results possible in unfolding the Bonner sphere data.

The input errors into BUNKI were obtained from the error in the coefficients from the weighted least-squares program. The sum of the errors for all the spheres was used to develop a weighting factor to determine the relative importance of each sphere data to the unfolding process. The difference between the measured and calculated spectrum was the error reported in the unfolding process and was used to represent the errors of the beryllium multiplication. The input errors are not directly propagated to the resulting output errors of the fluence.

The total particle fluence is relatively insensitive to choice of Bonner spheres. (The average energy of the unfolded spectrum did change depending on the selection of spheres). The Bonner sphere selection criteria used in this investigation were

1) a minimum of six of the eight Bonner spheres were used with at least one sphere selected that emphasized an energy range (i.e. low energy: bare detector, 5.08 cm or 7.62 cm moderating sphere, middle energy: 12.70 cm moderating sphere, high energy: 20.32 cm, 25.40 cm, 30.48 cm, or 45.72 cm moderating sphere), 2) sphere selection which provided the "best fit" to the experimental data as determined by the percent error listed in the final output. The multiplication value was obtained by dividing the total fluence with beryllium present by the total fluence without beryllium present. The error associated with the multiplication was obtained by simple error propagation techniques.[46]

Weighted Bonner Sphere Count-Rate Method

To determine the neutron multiplication, the weighted sum of count-rates due to the leakage spectrum from the beryllium shell were divided by the weighted sum of the count-rates due to the neutron source alone at the same location. This method involves using weighted Bonner sphere counts to obtain the total fluence at a location, or at least a value that differs from the total fluence by a multiplicative constant which is not spectrally dependent.[32]

One hundred seventy one group ANISN calculated leakage spectra were used to prove the validity and show the associated

uncertainty in the weighted-sphere method. The calculated neutron leakage multiplication is defined as

$$(29) \qquad M = L/S$$

where

$L \quad = \quad$ the calculated total leakage fluence obtained with the source inside the beryllium sphere,

$$(30) \qquad L = \sum_g X_g^L$$

where

$S \quad = \quad$ the bare source total fluence,

$$(31) \qquad S = \sum_g X_g^S$$

where X_g^L and X_g^S are the energy group fluence at the point of interest for the leakage neutrons and bare source neutrons respectively. The leakage fluences were taken from ANISN calculations, and the source fluences were based on multigroup source representations used in ANISN for the sources of interest.

In experimental measurements, the fluences at the specified

location were obtained by weighting the Bonner count-rate data. For the leakage fluence this is

$$(32) \qquad 1 = \sum_{i=1}^{N} C_i^L w_i$$

where

N = number of Bonner spheres used in the weighting scheme,

w_i = weight of the ith Bonner sphere,

C_i^L = room return corrected count-rate of the ith sphere,

and for the source fluence

$$(33) \qquad s = \sum_{i=1}^{N} C_i^S w_i.$$

To determine the weighting schemes and their associated uncertainties, the multigroup leakage and source fluence were folded into the chosen Bonner sphere response to estimate the count-rate as

follows:

(34)
$$C_i{}^S = \sum_g e_i \, X_g{}^S \, R_{ig}$$

and

(35)
$$C_i{}^L = \sum_g e_i \, X_g{}^L \, R_{ig}$$

where

R_{ig} = response of ith Bonner sphere in counts per unit neutron fluence for the gth group,

e_i = normalization factor for the response of the ith Bonner sphere.

The weights for a particular Bonner sphere combination can be obtained by solving any of several least-squares formulations of the weighting problem.[57] In this investigation, the weights that minimized in the least-squares sense the group-by-group difference in fluence was used, i.e.

(36)
$$(\Delta X)^2 = \sum_g (X_g - \sum_i C_i \, w_i)^2$$

where the normalization factor was set equal to unity. Eqn. (36) can be simplified to

$$(37) \qquad \sum_i (w_i R_{ig} - 1)^2$$

This least-squares problem was solved to determine the Bonner sphere combination and the associated weights to generate a pseudo equal-probability detector system. Additional constraints included: 1) the combination resulted in an acceptable total error in the multiplication for all sources and 2) all positive weights be used. Initially, the second constraint was specified to ensure that small differences between terms in Eqns. (32) and (33) did not cause a disproportionate increase in the relative error if certain spectral shapes were obtained.[57] Upon evaluation with the spectral shapes of interest, this constraint was dropped.[32]

The criteria for a level of total acceptable error was based upon the error in the "measured" multiplication given as

$$(38) \quad (\Delta m)^2 = \qquad [(M-m)^2]$$
$$+ 1/s^2 [\sum w_i^2 (C_i{}^L/t_i{}^L + 1^2 \, C_i{}^S/s^2 t_i{}^S)]$$
$$+ 1/s^2 [\sum w_i^2 d_i^2 \{(C_i{}^L)^2 + 1^2/s^2 (C_i{}^S)^2\}]$$

where

m = $1/s$ (the experimental multiplication),

$t_i{}^L$ = measurement time for the leakage for the ith sphere,

$t_i{}^S$ = measurement time for the source for the ith sphere,

d_i = calibration error associated with the response normalization factor.

This equation for error parallels that of Nachtigall and Burger[57] for using weighted Bonner sphere count-rates to obtain dose equivalent rates. The first bracketed term is the square of the error due to the method for determining the multiplication assuming no experimental errors exists. The second bracketed term is the square of the error due to counting statistics. The third bracketed term is the error associated with the normalization of the calculated responses to the experimental data. This normalization was performed with a calibrated ^{252}Cf source[37] with a value of 3.5% given to d_i.[32]

All possible three-, four-, five-, and six-ball combinations of the bare detector, 5.08 cm, 7.62 cm, 12.70 cm, 20.32 cm, 25.40 cm, 30.48 cm, and 45.72 cm Bonner spheres were tested for ^{252}Cf and DT sources in a 6.99 cm thick beryllium shell.[32] Only those meeting the specified maximum multiplication error for the sources of interest were investigated. The combinations chosen were shown in Table VII and Table VIII. The weighted responses may deviate sharply from a flat response on a group-by-group basis[57], but if they do so at energies of little importance in the leakage spectra, the multiplication may still be determined with a high degree of precision.[32] The largest contributing factor to the error in the "measured" multiplication was from the calibration error d_i rather than by the method error.

The values for the errors in measured multiplication varied between 3.8% to 7.5% for the four-sphere systems. When folded with the uncertainty in the actual source strengths (3.5%) the total error in the multiplication is of the order of 6% to 7%.

B. Source Spectra

Well characterized neutron source distributions are required to perform integral neutron cross section analysis. The neutron spectra from ^{252}Cf have been extensively studied and are well documented.[4,22,37,38,52] A measurement of a ^{252}Cf neutron

source with Bonner spheres was unfolded using the the neutron unfolding code BUNKI. The results shown in Fig. 12 with an average energy of 2 MeV closely resembles the an NBS calculated ^{252}Cf spectrum shown on the same plot.

Typically the DT neutron source is depicted in transport calculations as simply a spike in the 14 MeV range. An example of a bare DT measurement measured by Bonner spheres and unfolded by BUNKI is shown in Fig. 13.

C. Leakage Multiplication from Polyethylene

To establish the credibility of the Bonner sphere technique to measure integral cross sections it was necessary to compare measured results with a well established calculated reference. To do this several integral tests involving ^{252}Cf and DT neutrons inside polyethylene were performed. The unfolded spectra for these measurements can be seen in Fig. 14 and Fig. 15. The leakage fluence from the polyethylene spheres were compared to the source fluence shown above to obtain the measured neutron leakage multiplication shown in Table XIII.

A comparison of the leakage multiplication for polyethylene, as determined using BUNKI, versus the weighted sphere technique can be seen in Table XIV. BUNKI, because of its demonstrated ability to
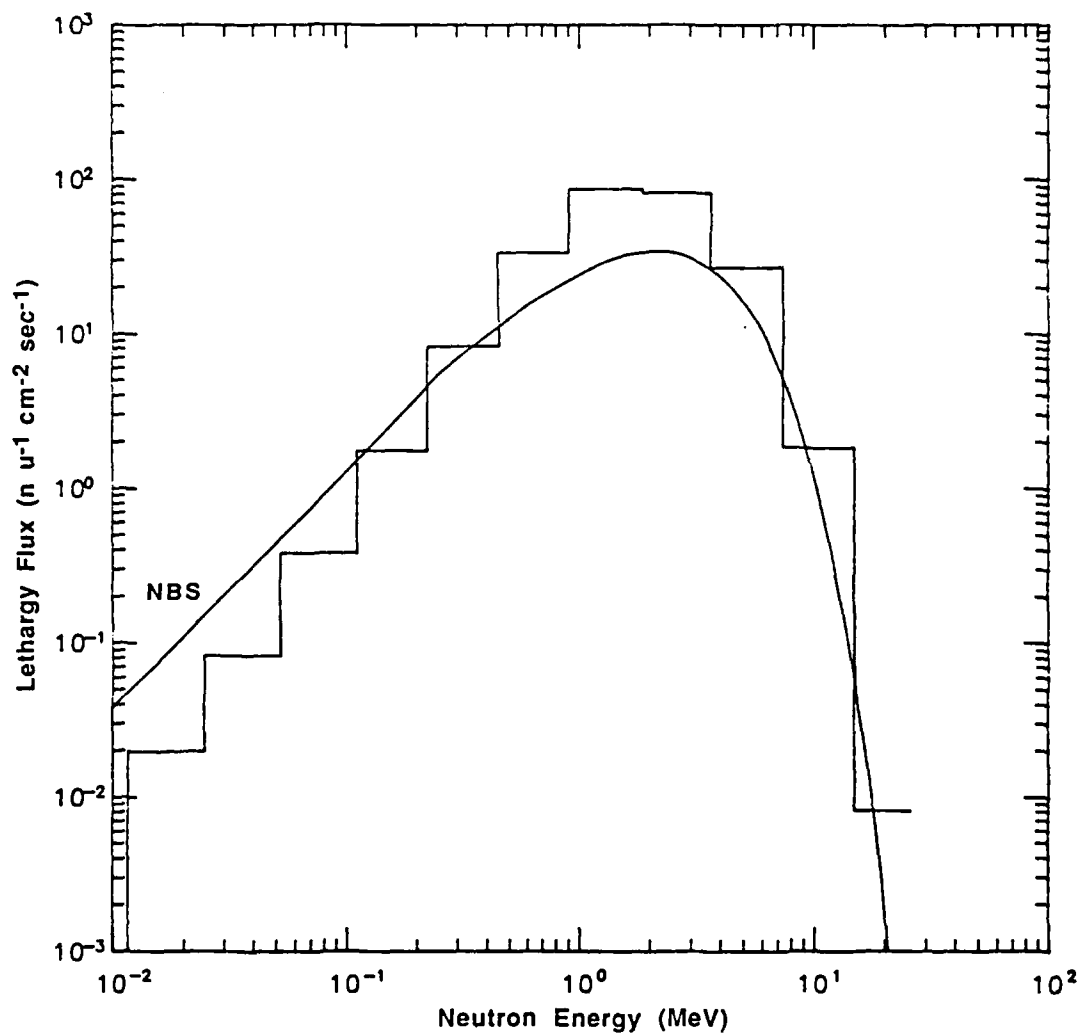
Fig. 12   BUNKI Unfolded ^{252}Cf Spectrum
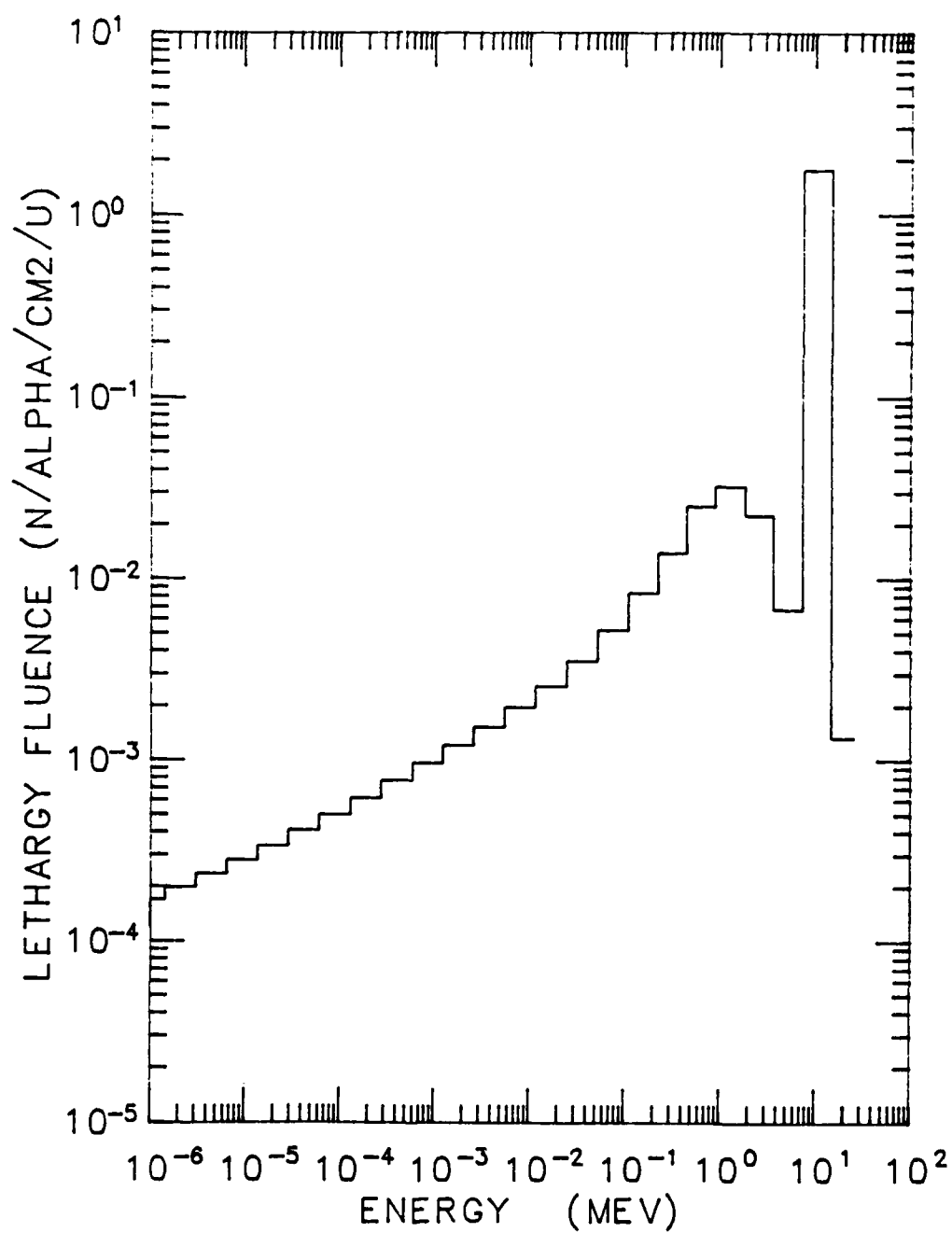
Fig. 13 BUNKI Unfolded DT Spectrum
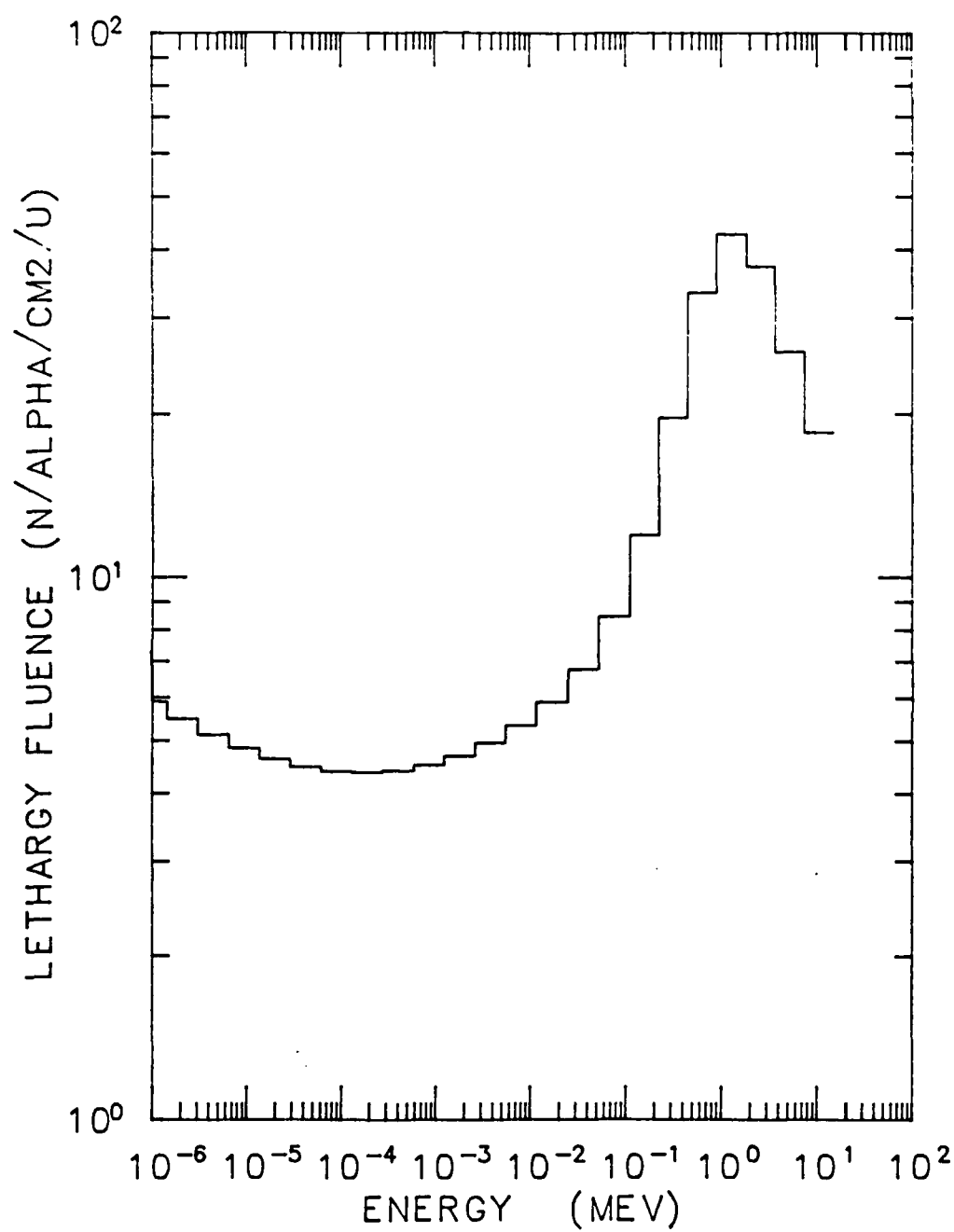
Fig. 14   BUNKI Unfolded ^{252}Cf in Polyethylene
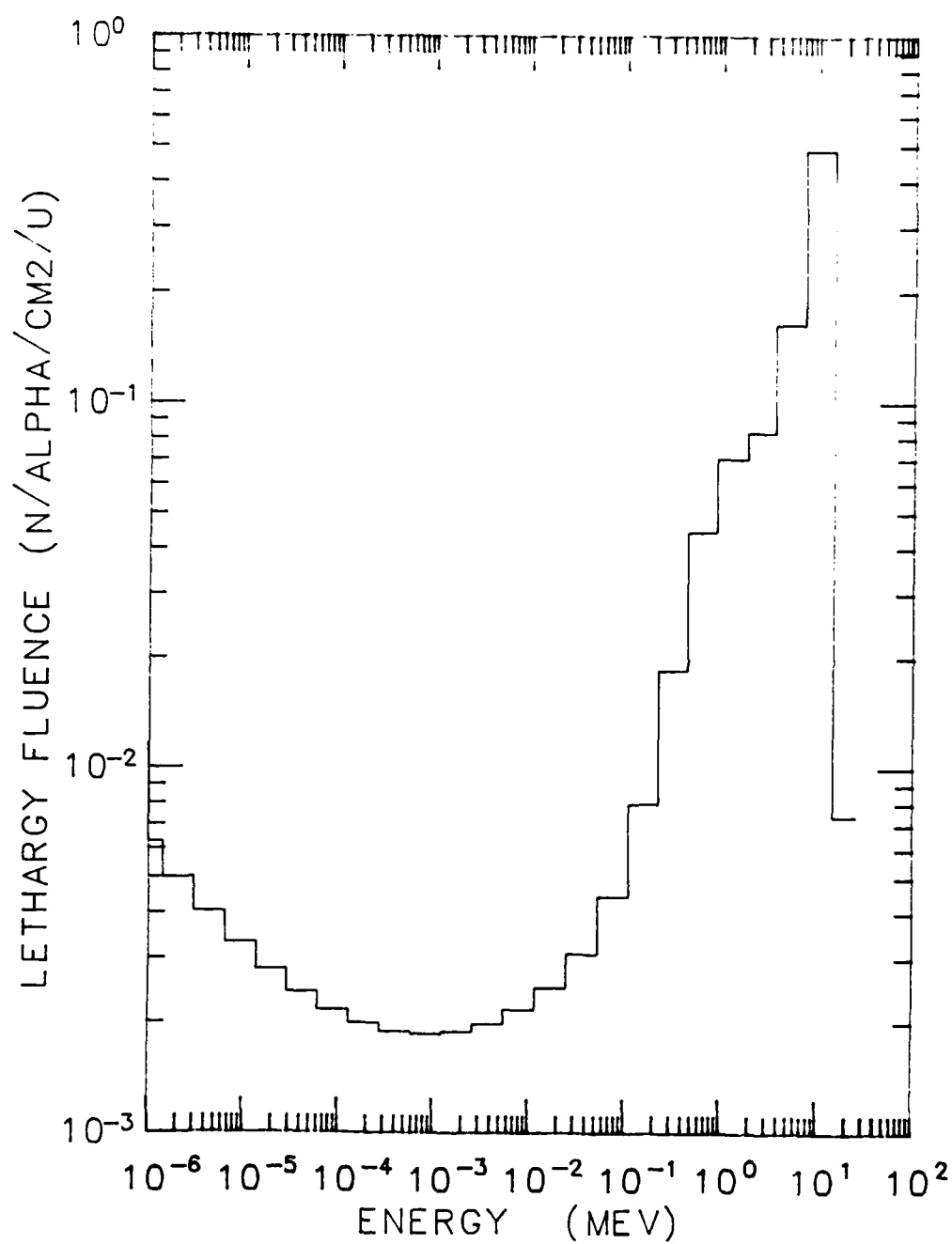
Fig. 15 BUNKI Unfolded DT in Polyethylene

TABLE XIII

LEAKAGE MULTIPLICATION FROM POLYETHYLENE

UT-Polyethylene for ^{252}Cf neutrons:

      ANISN (DLC-31):   0.0548

      ANISN (DLC-41):   0.0569

      Measured multiplication (distributed source) = 0.055(.003)

LLNL-Polyethylene for ^{252}Cf neutrons:

      ANISN (DLC-31):   0.4309

      ANISN (DLC-41):   0.4383

      Measured multiplication (distributed source) = 0.43(.03)

NCSU-Polyethylene for DT neutrons:

      ANISN (DLC-31):   0.5175

      ANISN (DLC-41):   0.5255

      Measured multiplication (distributed source) = 0.52(.03)

Numbers in parentheses represent one standard deviation in the measurement uncertainty.

TABLE XIV

WEIGHTED BALL VERSUS BUNKI COMPARISON
FOR POLYETHYLENE LEAKAGE MULTIPLICATION

Sphere	Multiplication		
	Measured		Calculated
	Wgt'd Ball	BUNKI	
UT-Cf	0.045(.003)	0.055(.003)	0.055
LLNL-Cf	0.39 (.02)	0.43 (.03)	0.431
NCSU-DT	0.45 (.03)	0.52 (.03)	0.518

The numbers in parentheses represent one standard deviation in the measurement uncertainty.

determine total neutron fluence to within several percent in health physics applications[33], was used to judge the weighted sphere technique. All measurement data which were compared to calculated data were obtained from BUNKI. The results indicate that the weighted sphere method, originally thought to be independent of the source spectra[32], is spectrum dependent. The weights for the ^{252}Cf polyethylene spectra were obtained by minimizing the group-by-group difference in fluence from a ^{252}Cf source in the 6.99 cm thick beryllium shell. The weights for the DT polyethylene spectra were obtained by minimizing the group-by-group difference from a DT source in the same beryllium shell. A larger differences between BUNKI and the weighted sphere technique are evident as the spectra differ from those used to determine the weights. This implies that the weights, which were determined for sources in a 6.99 cm beryllium shell, would have to be recalculated for each spectrum. This requires a knowledge of the leakage spectra for each measurement from which new weights would have to be generated. In light of the availability and flexibility of the neutron unfolding code BUNKI, the weighted sphere technique was not used in the analyses of beryllium neutron leakage.

The uncertainty associated with the BUNKI results mentioned above was obtained as noted in Appendix A. The 5.7% uncertainty was added in quadrature to the error of the BUNKI fit (typically between 0.3 - 1.2%) and then rounded off to obtain the value of 6.0%.

The relative number of neutrons in each of four energy groupings, 15-10 MeV, 10-2 MeV, 2 MeV-0.77 eV, 0.77 eV-thermal, for both the calculated (by ANISN using ENDF/B-IV) and unfolded-measured spectra can be seen in Table XV. This grouping was done to crudely determine the energy distribution of the leakage neutrons and to allow comparison of the calculated leakage spectra with those obtained by Wong et al.[19] for the 13.8 cm and 19.9 cm thick beryllium shells. The addition of the unfolded measured spectra allows one to see if the spectral shape obtained by BUNKI are close to those predicted by calculations. It is in no way used as a criteria to judge the correctness of the total energy-integrated fluence from BUNKI.

D. Leakage Multiplication from Beryllium

Neutron leakage multiplication for ^{252}Cf and DT neutron sources inside beryllium shells were measured. The results of these measurements are not directly comparable to most of the previous experiments because of the different geometries and sources used. In the case of Wong et al.[19] the same beryllium assemblies were used and the experimental results for DT neutrons should be comparable. The results for the 13.8 cm and 19.9 cm beryllium shell thicknesses as measured by Wong and the present research are shown in Table XVI. As can be seen Wong's measured value for both assemblies are much higher

TABLE XV

RELATIVE NUMBER OF NEUTRONS PER ENERGY GROUP

Spectrum	ENERGY			
	15-10 MeV	10-2 MeV	2 MeV-.77 eV	.77 eV > E
UT Poly-Cf	.009	.342	.280	.369
BUNKI	.066	.343	.323	.268
LLNL Poly-Cf	.004	.342	.349	.305
BUNKI	.057	.329	.476	.138
NCSU Poly-DT	.501	.260	.149	.090
BUNKI	.682	.087	.141	.090
4.6 cm Be-Cf	.002	.275	.722	.001
BUNKI	.007	.446	.547	.000
6.99cm Be-Cf	.002	.219	.776	.004
BUNKI	.038	.275	.664	.023
13.8 cm Be-Cf	.001	.096	.713	.190
BUNKI	.033	.150	.711	.106
19.9 cm Be-Cf	.001	.048	.519	.432
BUNKI	.000	.086	.584	.330
4.6 cm Be-DT	.621	.130	.249	.000
BUNKI	.556	.112	.332	.000
6.99cm Be-DT	.500	.164	.334	.002
BUNKI	.439	.142	.404	.015
7.85cm Be-DT	.429	.183	.363	.025
BUNKI	.324	.200	.430	.046
9.39cm Be-DT	.396	.161	.432	.011
BUNKI	.284	.265	.441	.010
13.8 cm Be-DT	.251	.148	.495	.106
BUNKI	.240	.173	.519	.068
WONG	.307	.227	.402	.064
19.9 cm Be-DT	.146	.119	.474	.261
BUNKI	.117	.117	.566	.200
WONG	.159	.185	.418	.231

TABLE XVI

COMPARISON OF EXPERIMENTAL VALUES
FOR SAME BERYLLIUM ASSEMBLIES

Inner Radius (cm)	Shell Thickness (cm)	Multiplication	
		PRESENT RESEARCH	WONG ET AL. RESULTS
8.00	4.6	1.43(.09)	
8.00	13.8	1.50(.09)	1.80(.180)
8.00	19.9	1.52(.09)	1.95(.195)

The numbers in parentheses represent one standard deviation in the
measurement uncertainty.

*   - All calculated data represent 1-D modeling.

** - ENDF/B-IV

*** - ENDF/B-V/LANL

than the same neutron leakage measured in the present research. Since an intimate knowledge of Wong's experiment was not known an exhaustive investigation was performed to determine if an incorrect assignment of a variable or assumption in the original model of the present research could be responsible for the noted discrepancy.

Applicability of the ESJ Model

The first test involved the applicability of the original model of Eisenhauer, Schwartz, and Johnson for room-return correction. According to Johnson[62] the ESJ model is applicable to neutron sources of any energy as long as the $1/r^2$ law is applicable. Hunt[21] stated that a test of the stability of this technique involves performing repeated least-squares fits, each time deleting the point nearest the the source. If the values computed for the gradient and the intercept are stable as a function of the measurement range then "both the measurements and the method of analysis must be presumed correct".[21]

This test was applied to two extreme ranges of spectra, DT neutrons in 3.5 mfp beryllium and a bare DT neutron source. The results are shown in Appendix E. In each instance the method proves to be stable and the ESJ model appears to be applicable for this investigation.

One can also see from Tables E.1 and E.2 that the room-return correction varies for each Bonner sphere. The correction for room scattered neutrons varies from about 67% for the 5.08 cm diameter Bonner sphere with DT neutrons in the 19.9 cm thick beryllium shell to about 10% for the 30.48 cm diameter Bonner sphere for the bare DT source. Using the data from all the Bonner spheres and unfolding the spectra using BUNKI this translates into a 36% room-return correction for the 19.9 cm thick beryllium shell and a 21% correction for the bare DT source. As expected the room-return corrections vary according to the source spectra with less correction occurring for the harder spectra. The beryllium neutron leakage multiplication obtained using no room-return correction is shown in Appendix G. As one would expect from above the leakage multiplication increases by the percent difference in room-return correction between the beryllium leakage spectrum and the bare DT source (Table G.1). This causes the measured leakage multiplication for the thinner shells to be higher than that calculated by either ENDF/B-IV or ENDF/B-V/LANL. This is an incorrect trend because, regardless of which cross section set is being used to calculate the leakage multiplication, one would expect the measured values for the thin shells to most closely approach the calculations for the thinner shells.[14] Therefore, determining the multiplication using raw count-rate data uncorrected for room-scattered neutrons would not be valid.

Variations of Variables in ESJ

The next series of tests pertain to the variables used in the ESJ model, in particular the values for the air-scatter coefficient A, the values for the distributed source correction factor $F_1(D)$, and the values for the source-detector separation distance D_0.

Since the values for the air-scattered coefficient were not recomputed for each neutron source-beryllium sphere combination it was necessary to determine the maximum effect variations could have on the multiplication. The values for A for the bare DT source came from values generated for AmBe neutron sources [21] with an average energy of 4.5 MeV. [22] A computed value of A for a DT source would not be expected to be different from this value by more than a factor of 6 (based on variations in A for ^{252}Cf to AmBe with linear extrapolation to 14 MeV). For this test the value of A was decreased by a factor of 10 causing a change in total fluence less than the measurement uncertainty (Appendix D).

The values of A for DT neutrons in beryllium were also those obtained from the AmBe source. Variations in A for a moderated source are expected to increase no more than a factor of 3 (based upon variations in A for AmBe to that for D_2O moderated ^{252}Cf). The test was repeated this time by increasing the value of A by a factor of 10. The change in fluence after unfolding was again less than the 6% measurement uncertainty.

The overall observation from this test is that there is no statistically significant change in the multiplication for variations in A of a factor of 10.

The next test was to determine the impact of using the distributed source correction factor versus the point source correction factor for beryllium spheres used in the measurements. The largest effect would occur for the 19.9 cm thick beryllium sphere (Table IX). Here the leakage multiplication determined by using the distributed source correction is 2% lower than that obtained with a point source correction factor. Although this increases the discrepancy between the present measurement and the measurement of Wong et al.[19] it does not in itself contribute to the large variation in multiplication and based upon the polyethylene studies is required.

The uncertainty in determining the source-detector distance was set at 3 mm. This value was based upon using a laser to align the target assembly inside the spheres and the precision with which the detector could be repeatedly replaced in the measurement room. To investigate the maximum variation in multiplication one would expect, the count-rate data for a bare ^{252}Cf source was unfolded for the correct values of D_0, then reprocessed with the values of D_0 varied by 2 cm. The results indicate a maximum variation in multiplication of 4.2% result (Appendix H).

Choice of Response Matrix and Air Attenuation

There was originally some concern as to the selection of the proper response matrix (between UTA4 and SAN4) and to whether a problem of air attenuation greater than what was accounted for in the "A" factor used in the ESJ model existed. According to Johnson[52] no more than a 15% variation was expected regardless of which response was chosen. This may have been true for the neutron spectra in his investigation but larger variations (up to 26%) were found to exists for very soft spectra ($<E>= 300-700$ keV) as for the ^{252}Cf in 19.9 cm beryllium. The variations, with UTA4 always predicting a fluence lower than SAN4, decreased as the spectra became harder with no significant variations observed for the DT source in the 4.6 cm thick beryllium shell. To aid in choosing the most appropriate response the count-rate data from neutrons leaking out of polyethylene were unfolded and the results compared to calculated values. From this study it was determined that UTA4 came within 1.0% of the calculated leakage multiplication (leakage neutron per source neutron) whereas SAN4 overpredicted by 16-19%. Because the total fluence of these spectra, with an average energy lower than most of the beryllium spectra measured, was correctly determined by UTA4 with its corresponding sphere correction factors, it was the response chosen for all analyses.

It was also postulated that for the neutron sources inside thicker shells with severely degraded energy spectra that perhaps air attenuation in excess of that accounted for by the air-scatter coefficient in the ESJ model existed. This was ruled out by the polyethlyene measurements because the average energy of their leakage neutrons were lower than those for beryllium (Table XV).

Summary of Tests and Validity of Experimental Data

The previous tests were performed to study the effect of the major assumptions used in the development of the measurement technique. In each case their effect cannot attribute to the discrepancies noted. As far as the actual experimental data most points were measured more than once by different experimenters on different days with no total fluences disagreeing by more than 8%. Each multiplication data point represents a minimum of 77 individual measurements which were then processed through a least-squares program. The possibility of obtaining a bad neutron leakage multiplication data point from a poor measurement is minimal. In each case the number of neutrons detected per alpha was monitored by two external flux monitors. The stability of the internal flux monitor was within 7%. Targets were never used much beyond 1 Ma-hr burnup at which point the contamination of DD neutrons in the total neutron yield is 1%.

Chapter V Calculational Analyses and Results

The beryllium leakage multiplication were calculated using
the one-dimensional discrete-ordinates codes ANISN[63] and
ONEDANT[64] with ENDF/B-IV[65] and ENDF/B-V[53] with Los Alamos
National Laboratory (LANL) revisions[2] (ENDF/B-V/LANL),
respectively. The effect of the reentrant hole on the leakage
spectrum could not be taken into account; however, its effects have
been shown to be negligible at the measurement locations used.[4]

Calculations were performed with ANISN for polyethylene
spheres to provide a computational benchmark[7,19] to which the
present measurement technique could be compared.

Calculations were then performed for beryllium, whose cross
sections are not as well known[5,6,9,17,19], to provide calculated
data to compare against the present experimental results. The
beryllium spheres of 13.8 cm and 19.9 cm wall thickness had
hemispherical shells missing between $12.6 \leq r \leq 20.1$ cm. Although
quantitative results for these assemblies were obtained using
one-dimensional calculations, exact modeling using either a
multidimensional discrete ordinates code or a Monte Carlo code would
be necessary to provide calculated results directly comparable with
the experimental data. The scope of the present research was to
develop a technique to make integral measurements using Bonner

104

spheres and to use this technique to obtain information about the multiplication properties of beryllium. The information obtained from the complete shell configurations fulfilled this requirement and hence only one-dimensional analyses were performed. The one-dimensional calculations provided a comparison of the leakage multiplication predicted from ENDF/B-IV and ENDF/B-V/LANL, provided a comparison of the leakage multiplication for various size internal void radii, and provided information about how well the cross sections represent the experimental results.

A.   Calculations using the ANISN Transport Code

Neutron leakage spectra for the polyethylene and the beryllium spheres were modeled using ANISN.[63] ANISN is a one-dimensional, time-independent, multigroup, discrete ordinates code which solves the Boltzmann transport equation using finite differences for discrete angular and spatial values. The transfer cross sections were expanded in a series of Legendre polynomials and the expansion coefficients were incorporated into tables. One transfer table was required for each order of the Legendre expansion.

All ANISN runs were performed with $S_{16}P_3$ using 100 spatial mesh intervals. Two coupled neutron and gamma-ray multigroup cross section sets were used for the polyethylene and beryllium

calculations.

The DLC-31/(DPL-1/FEWG1) cross section set[66] and the DLC-41/Vitamin C multigroup cross section set[67] were used for the polyethylene calculations.

DLC-31 is a 37 neutron group, 21 gamma group cross section set for 35 nuclides which was developed for the Defense Nuclear Agency. The library is based on cross-section data from the DNA Working Cross Section Library and the ENDF/B-IV. The group structure covers the neutron energy range between 10^{-11} eV to 19.64 MeV weighted by a 1/E with a thermal group Maxwellian weighting spectrum with a 300°K temperature.

DLC-41 is a 171 neutron group, 36 gamma group cross section set with a group structure which covers the neutron energy range between 10^{-5} eV to 17.333 MeV. The set was generated from ENDF/B-IV for a weighting function which consisted of a Maxwellian from 10^{-5} eV to 0.125 eV, a 1/E shape from 0.125 eV to 820.8 keV, a fission spectrum from 820.8 keV to 10 MeV, a 1/E shape from 10 MeV to 12.57 MeV, a velocity exponential fusion peak from 12.57 MeV to 15.57 MeV, and a 1/E shape above 15.57 MeV.[4] This weighting function was designed to cover a wide range of applications to include fusion neutron spectra.

B. Calculations using the ONEDANT Transport Code

ONEDANT[64] also was used to calculate leakage from the

beryllium shells. ONEDANT is a one-dimensional multigroup discrete ordinates code which solves the steady-state form of the neutral-particle Boltzmann transport equation in plane, cylindrical, spherical, and two-angle plane geometries. Both regular and adjoint, inhomogeneous and homogeneous problems with vacuum, reflective, periodic, white albedo, or inhomogeneous boundary flux conditions can be solved. General anisotropic scattering and anisotropic inhomogeneous sources are allowed. The discrete ordinates approximation is used to treat the angular variation of the particle distribution. The phase space is discretized using the diamond-difference scheme. Negative fluxes are eliminated by a local set-to-zero-and-correct algorithm with a standard inner (within-group) iteration, outer (energy-group-dependent source) iteration technique being used. Both the inner and outer iterations are accelerated using the diffusion synthetic acceleration method. ONEDANT has a modular structure to allow separation of the input and output functions from the calculational section. Sequential binary data files are used to transmit data between the modules. The cross sections used in these analyses were obtained from the MATXS cross section library.[68]

The MATXS libraries are produced from evaluated nuclear data in the ENDF/B format using the NJOY nuclear data processing system.[68] The MATXS library has 30 neutron groups with the most current LANL revisions for the beryllium neutron cross sections. The library includes

neutron data, photon data, self-shielding data, and thermal data in one package.

The MATXS library was interfaced with ONEDANT using TRANSX-CTR.[69] TRANSX-CTR reads evaluated nuclear data from libraries in the MATXS format and produces transport tables compatible with many discrete ordinates and diffusion codes. Neutron, photon, and coupled transport tables can be produced. Options in TRANSX include adjoint tables, self-shielding, mixtures, homogenization, group collapse, thermal upscatter, steady-state or prompt fission, elastic removal corrections, and various response-function edits. TRANSX uses interface files for cross-section input, flux input, and cross section output. The cross section output generated for use in ONEDANT was in the FIDO format.[64]

C.   Leakage Multiplication for Polyethylene

To establish the credibilty of using Bonner spheres to perform integral tests of cross sections of an unknown material, it was first necessary to demonstrate their ability to make integral measurements of a known material. The material chosen for this validation was polyethylene. The theoretical cross sections of polyethylene have been experimentally verified[7,19] and calculated neutron leakage multiplication based upon these cross sections provided a baseline to evaluate the validity of the present

measurement technique.

The neutron leakage spectra calculated by ANISN with DLC-31[66] for the ^{252}Cf source and DT neutron source in the LLNL and the NCSU polyethylene spheres are shown in Fig. 16 and Fig. 17, respectively. The computed leakage multiplication for these spheres, previously shown in Table XIII, were determined using the densities shown in Table VI. The polyethylene surrounding the ^{252}Cf produce a neutron leakage spectra with a major protion of the leakage neutrons between thermal to 2 MeV (Table XV). The ability to accurately measure neutrons in the thermal to 2 MeV range was important because thick shells of beryllium also produce energy degraded leakage spectra in the same range. In the past this has resulted in a larger calculational uncertainty for thick blankets because no low-energy spectral measurements were available to compare with calculated values.[14]

D. Leakage Multiplication for Beryllium

ANISN with ENDF/B-IV and ONEDANT with ENDF/B-V/LANL were used to calculate the neutron leakage for the ^{252}Cf and the DT neutron sources in the beryllium shells. ANISN/DLC-41 calculated leakage spectra from ^{252}Cf neutrons in the 6.99 cm thick beryllium shell is shown in Fig. 18. The calculated neutron leakage multiplication from ^{252}Cf and DT neutrons in beryllium provided a comparison
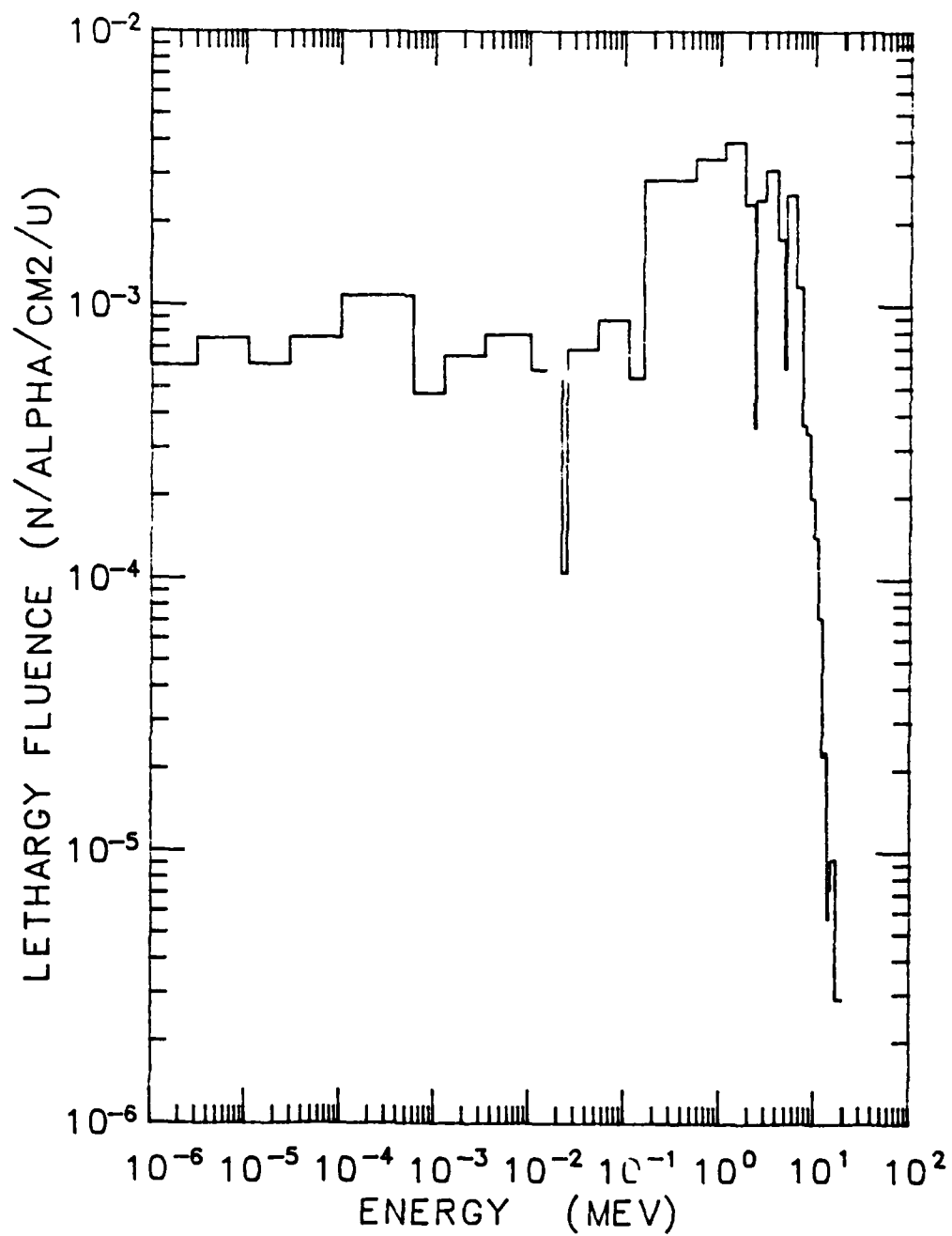
Fig. 16 ANISN Calculated Leakage for ^{252}Cf in Polyethylene
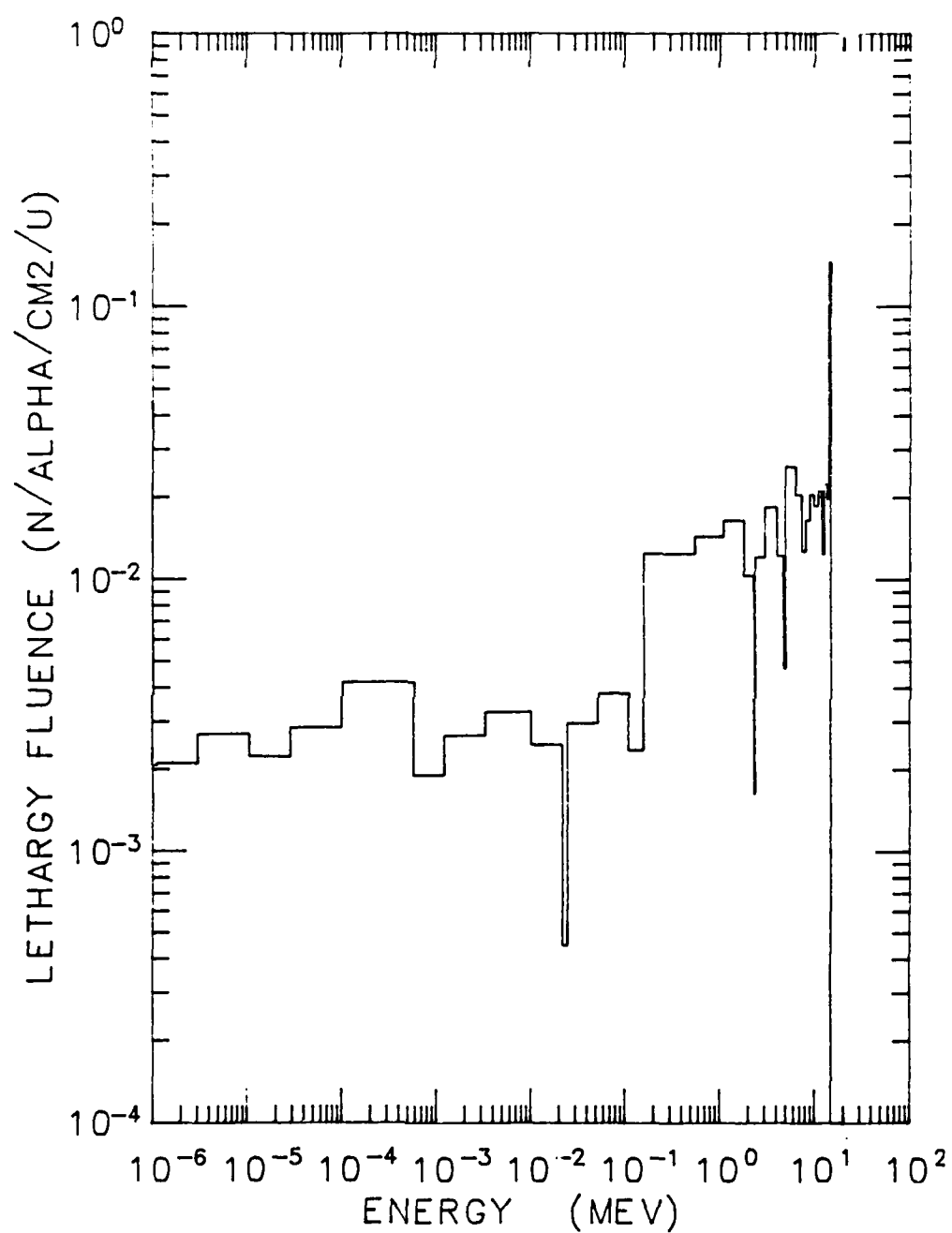
Fig. 17 ANISN Calculated Leakage for DT in Polyethylene
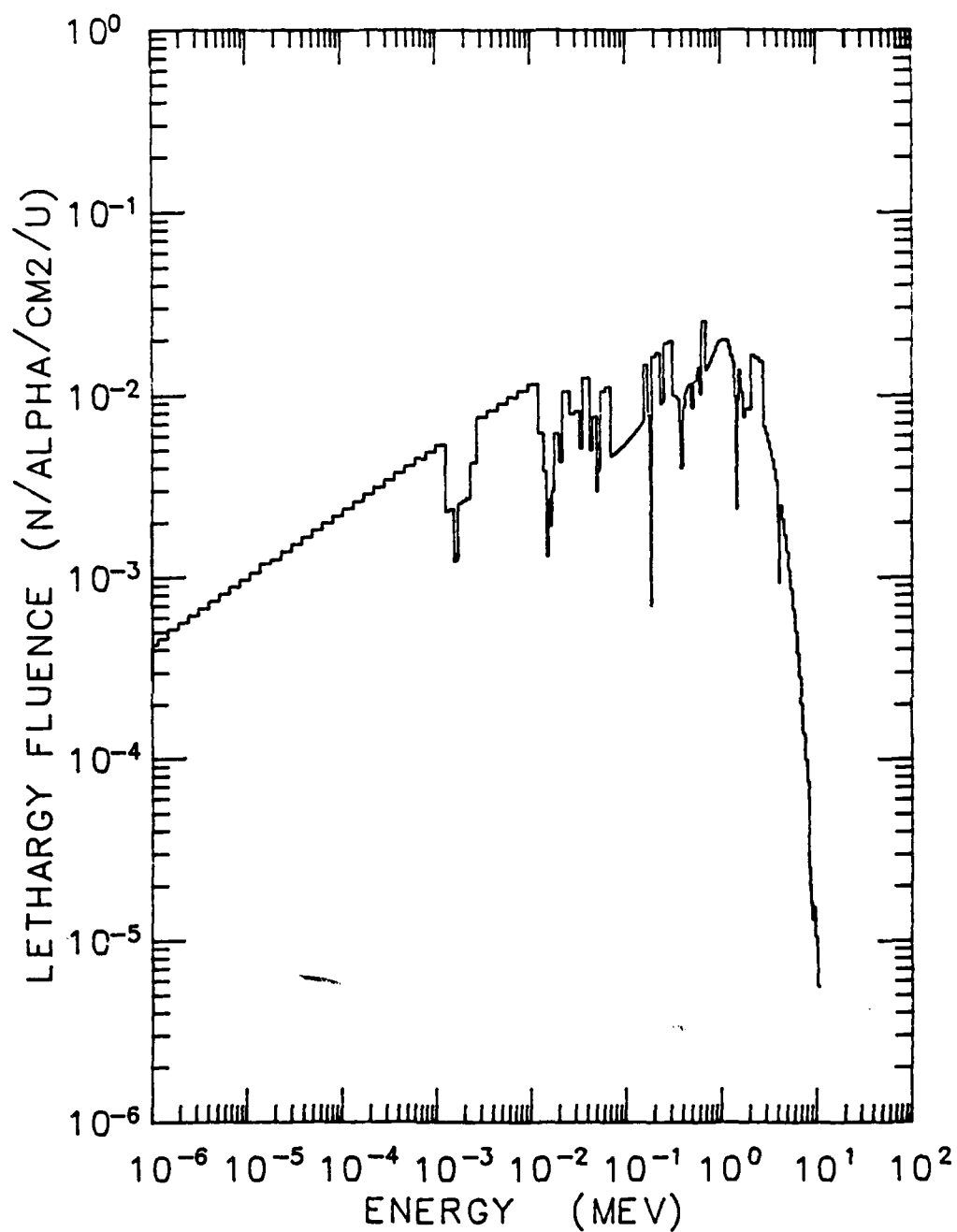
Fig. 18 ANISN Calculated Leakage for ^{252}Cf

in 6.99 cm Beryllium

of ENDF/B-IV and ENDF/B-V/LANL, allowed a study of the effect of the size of the internal void radii on the multiplication, and provided data to compare with the measured results. The calculated leakage multiplication for the beryllium shells are shown in Table XVII.

The calculated leakage multiplication from ENDF/B-IV were compared with that from ENDF/B-V/LANL to observe the effect of the current LANL revisions on the cross sections. The LANL cross section revision uses inelastic excitation levels to numerically account for the secondary neutron distribution.[2,8] Integrating the differential cross section over scattering angle in this evaluation yields the same values for the total $^9Be(n,2n)$ cross section as found in ENDF/B-IV and ENDF/B-V. Only the energy-angle correlation for the $^9Be(n,2n)$ cross section was changed.[2] This more correct secondary energy-angle correlation tends to produce lower energy and more forward peaked secondary neutrons. Isotropic scatter of the secondary neutrons was assumed in ENDF/B-IV AND ENDF/B-V.

The effect of the LANL ENDF/B-V revisions to the beryllium cross sections for neutrons from ^{252}Cf can be seen in Table XVII. As expected there is minimum change in the calculated multiplication for shell thickness up to 9.43 cm (2 MFP for ^{252}CF neutrons). For these thinner shells the effect of the more forward peaked secondary neutron distribution does little to reduce the calculated multiplication. For shells of these thicknesses ENDF/B-IV is expected to correctly predict the leakage multiplication because the total

TABLE XVII

COMPARISON OF ENDF/B-IV AND ENDF/B-V/LANL
CALCULATED LEAKAGE MULTIPLICATION FOR BERYLLIUM SHELLS*

Inner Radius (cm)	Shell Thickness (cm)	Multiplication					
		14 MeV			^{252}Cf		
		B-IV **	B-V ***	IV/V	B-IV	B-V	IV/V
8.00	4.6	1.28	1.32	0.97	1.04	1.00	1.04
3.17	6.99	1.41	1.46	0.97	1.05	1.01	1.04
20.06	7.87	1.52	1.55	0.98	1.05	1.00	1.05
3.17	9.43	1.55	1.61	0.96	1.06	1.00	1.06
8.00	13.8	1.83	1.84	0.99	1.06	0.97	1.10
8.00	19.9	2.09	1.97	1.06	1.03	0.89	1.15

*   - Calculated using 1-D models.

**   - ENDF/B-IV

**   - ENDF/B-V/LANL

cross section for thin shells of beryllium for fission neutrons has been well characterized from the numerous thermal reactor criticality experiments. For the thicker beryllium shells there is a significant change in calculated multiplication between ENDF/B-IV and ENDF/B-V/LANL. The leakage multiplication as calculated by ENDF/B-IV essentially stays constant up to the 19.9 cm thickness (4.4 MFP). This is contrary to what one expect with the average energy of the ^{252}Cf neutrons being lower than the 2.69 Mev threshold for the (n,2n) reaction where scatter and absorption are expected to dominate. The leakage multiplication as calculated by ENDF/B-V/LANL decreases for the thicker beryllium shells because the corrected secondary energy-angle correlation tends to produce preferentially forward peaked secondary neutrons with lower energy which fall below the (n,2n) threshold.

The effect of the LANL ENDF/B-V revisions to the beryllium cross section for DT neutron sources can also be seen in Table XVII. For shell thickness up to 13.8 cm (2.42 MFP for DT neutrons) ENDF/B-V/LANL predicts about the same leakage multiplication as ENDF/B-IV. It is not known if the difference is a true difference or just a statistical fluctuation in the calculations. One would expect the least amount of difference between the two cross sections for the thinner shells because the forward peaked secondary neutrons would have little effect on reducing the leakage multiplication before escaping from the shell.

For shells thicker than 13.8 cm the leakage multiplication predicted by ENDF/B-V/LANL is less than that calculated by ENDF/B-IV. This is expected because the secondary neutrons are more forward peaked and are transported through the beryllium with fewer chances of interaction.[2]

The next study using the calculated leakage multiplication involved the effect of the size of the internal void radius on the leakage multiplication. It has been shown that neutron leakage multiplication varies with the size of the internal void of the beryllium.[14] Since the various shell configurations used in the present experiments had different internal void radii (Table VI) an investigation was performed to study the effect of the internal void radii on the neutron leakage multiplication. The study was done using ONEDANT with ENDF/B-V for the three internal void radii used in the experiments (3.17 cm, 8.0 cm, and 20.06 cm) with the shell thicknesses varying from 4.6 cm to 19.9 cm. The results are shown in Table XVIII. By comparing these results with those calculated with ENDL 84 by Perkins[14] it can be seen that there is indeed a 3% increase in multiplication with increasing void radii for shell thicknesses less than 10 cm and a decrease in multiplication for increasing void radii for shells thicker than 10 cm. Perkin's neutron multiplication variations with void radii are of the order of a few percent compared to 18% in the present study for the 19.9 cm thick beryllium shell.

TABLE XVIII
INTERNAL VOID RADII INVESTIGATION
FOR DT NEUTRONS

MFP	THICKNESS (cm)	ENDF/B-V CALCULATED NEUTRON LEAKAGE MULTIPLICATION		
		I.R. = 3.17cm	I.R. = 8.0cm	I.R. = 20.06cm
0.8	4.6	1.34	1.36	1.38
1.22	6.99	1.52	1.54	1.57
1.37	7.88	1.59	1.61	1.61
1.64	9.43	1.69	1.69	1.69
2.10	12.0	1.81	1.78	1.72
2.42	13.8	1.86	1.79	1.70
2.96	17.0	1.85	1.73	1.58
3.5	19.9	1.76	1.61	1.44

The point of studying the variations in leakage multiplication as a function of void radii is to determine whether the thickness of beryllium alone is adequate to compare multiplication or whether a parameter such as mean chord length is necessary to represent the effective thickness of the neutron multiplier. As can be seen in Table XVIII the effect of the void radius is only of the order of a few percent for spheres less than 9.43 cm thick but for shells greater than this thickness the size of the internal void becomes an important factor. This indicates that the leakage multiplication of other individuals (Table V) are not directly comparable even if the same thicknesses of beryllium were used.

The effect of the variations in internal void radii, from 3.17 cm to 20.06 cm, on the leakage multiplication in the present research should be minimal. The large variations occur for beryllium thicknesses less than 9.4 cm so that the leakage multiplication reported should be on an equal basis (within 2-3%).

Chapter VI   Integral Analyses and Results

Bonner spheres are heavily used in health physics applications but have not yet been used in integral tests of cross sections. Therefore, the main emphasis of the present research was to develop the technique of integral measurements using a Bonner sphere spectrometer and to use the technique to extract information about the neutron multiplication properties of beryllium.

The proposed technique was tested by measuring samples of known cross sections (polyethylene).[7,19] These tests were in effect the proof-of-principle that Bonner spheres, with the appropriate models for background subtraction and spectrum unfolding, can be used to make integral measurements for leakage neutrons in the thermal to 14 MeV energy range.

Upon validating the technique, measurements of the neutron multiplication properties of beryllium were performed. These experimental results were used to test the adequacy of the most current beryllium cross sections available (ENDF/B-V/LANL).

A.   Comparison of Measurements and Calculations

Neutron leakage multiplication for ^{252}Cf and DT neutron

119

sources at the center of spheres of polyethylene and beryllium have been measured and calculated. Measurements were performed using a Bonner sphere spectrometer at 0° and 45° relative to the incident deuteron beam at distances from the source between one to two meters. The room- and air-scattered neutrons were removed by applying the model of Eisenhauer, Schwartz, and Johnson.[21] The multiplication was determined by dividing the total fluence, obtained by spectrum unfolding, with the material of interest in place by the total fluence obtained from the bare source.

The calculated leakage multiplication for polyethylene shells were determined using ANISN with DLC-31 and DLC-41. The leakage multiplication for the beryllium shells were determined using ANISN with DLC-41 (ENDF/B-IV) and ONEDANT ENDF/B-V/LANL. A direct comparison the 13.8 cm and 19.9 cm thick beryllium shells would require the use of a multidimensional code; however, in this investigation only one-dimensional analyses were performed.

B. Integral Tests of Polyethylene - Proof-of-Principle

The proof of the validity of the Bonner sphere technique for integral measurements was obtained by comparing the measured neutron leakage multiplication from polyethylene to the calculated leakage

multiplication for polyethylene. Polyethylene has well established cross sections.[7,19] The use of a well known material with well characterized sources such as ^{252}Cf[4,22,37,38,52] and DT neutrons provided sufficient data to justify the validity of the Bonner sphere technique for integral measurements. Three polyethylene spheres with ^{252}Cf and DT neutrons at their centers were used for the validation. A comparison of the measured neutron leakage multiplication with the calculated leakage multiplication were shown in Table XIII. The measured results were based on using the distributed source correction factor and the University of Texas response matrix, UTA4, with individual sphere correction factors. As can be seen the measured results are within one percent of the calculated results demonstrating the viability of the Bonner sphere technique for integral tests of cross sections.

The outcome of polyethylene measurements not only verified the measurement technique but showed that the shape of the Bonner sphere response and the individual sphere correction factors, which normalize the reponse to experimentally obtained neutron spectra, are correct in the thermal to 14 MeV energy range. This is the energy range of interest for evaluating the neutron leakage multiplication properties of beryllium.

By using Bonner spheres only one detection system was required for the entire energy range of interest (thermal to 14 MeV).

This simplified the experiment and the resulting analyses. Using a single detection system reduces the chance of detector efficiency mismatch when multiple detectors are used. For the thick beryllium shells a large fraction (upwards to 57%) of the leakage neutrons are below 0.77 eV requiring a detection system that provides reliable results for low energy neutrons. The only technique comparable to the Bonner sphere spectrometer in all these attributes is the manganese sulfate bath technique.[15]

C. Integral Tests of Beryllium Cross Sections

Upon demonstrating the Bonner sphere technique could reliably determine the neutron leakage multiplication of a known material it was used to determine the leakage multiplication of beryllium, whose theoretical cross section representations have not been fully confirmed by experiment.[5,6,9,14,19]

To test the cross sections for the entire energy range from thermal to 14 MeV, two beryllium experiments were performed. The first involved using ^{252}Cf with about 66% of its neutrons emitted below the 2.69 MeV threshold energy of the 2.43 MeV excitation level for the (n,2n) reaction. The 2.43 level represents one of the strongest transitions of ^{9}Be with little excitation being observed for the 1.68 MeV level.[14] The percentage of neutrons below the

(n,2n) threshold increases for the thicker beryllium shells as the energy of the leakage neutrons decrease from elastic scatters with the beryllium. This experiment, especially when applied to the thicker beryllium shells, tested the adequacy of the representations for the absorption reactions in addition to the (n,2n) reactions. Experiments with ^{252}Cf were performed for the 4.6, 6.99, 13.8, and 19.9 cm thick beryllium shells. A comparison of the measured and calculated neutron multiplication is shown in Table XIX.

When compared to the present measurements the ENDF/B-IV calculated multiplication for ^{252}Cf in beryllium underestimates the leakage multiplication for the 4.6 cm beryllium shell (1.0 MFP for ^{252}Cf) while overpredicting the multiplication for the 13.8 cm and 19.9 cm shells (3.1 and 4.4 MFP respectively). The calculated multiplication for the 13.8 cm and 19.9 cm shells in Table XIX are based on one-dimensional calculations, with the full beryllium thickness used, and as such are not directly comparable with the experimental results.

The above comparison of the ENDF/B-IV ^{252}Cf calculations to the experimental results indicate several discrepancies. First as previously mentioned ENDF/B-IV predicts a lower leakage multiplication than was experimentally measured for the 4.6 cm thick shell. The evidence previously shown leans to the fact that the total cross section for a shell of this thickness for fission neutrons are well

TABLE XIX

COMPARISON OF THE CALCULATED TO EXPERIMENTAL (C/E)
LEAKAGE MULTIPLICATION FOR BERYLLIUM SHELLS WITH ^{252}Cf*

Inner Radius (cm)	Shell Thickness (cm)	Multiplication				
		EXPERIMENT	B-IV **	C/E	B-V ***	C/E
8.00	4.6	1.22(.07)	1.04	0.85	1.00	0.82
3.17	6.99	1.04(.06)	1.05	1.01	1.01	0.97
8.00	13.8	0.93(.06)	1.06	1.14	0.97	1.04
8.00	19.9	0.67(.04)	1.03	1.54	0.89	1.33

The numbers listed in parentheses represent one standard deviation in the measurement uncertainty.

* - All calculated data represent 1-D modeling.

** - ENDF/B-IV

*** - ENDF/B-V/LANL

known. Any corrections, within the constraint that the total cross
section remain unchanged, that could be made as far as the forward
scatter of secondary neutrons will not effect the multiplication of
this 1.0 MFP shell. This implies that if a correction were to be made
to the partial cross sections it would have to involve increasing the
(n,2n) cross section of the 1.68 MeV level, currently 0.03 barns, at
the expense of the (n,alpha) cross section, currently 0.08 barns. The
effect of making a change within the constraint of maintaining the
same total cross section on the multiplication can not be determined
without sensitivity analysis. Before any serious changes are
undertaken; however more measurements on shells of the same or
comparable thickness need to be done to ensure the noted trend is well
documented. The second discrepancy occurs in the calculated
multiplication for 13.8 cm and 19.9 cm thick beryllium shell
assemblies. There seem to be serious problems with either the
1.68 MeV or 2.43 MeV (n,2n) transitions or the (n,alpha) reaction.
Previous work by Drake et al.[7,53] indicated that from about 6 to
12 MeV, the cross section for the excitation of the 2.43 MeV level for
beryllium in ENDF/B-IV should be lower by up to a factor of two. This
change could be made by altering the energy-angle correlation, as was
done in ENDF/B-V/LANL, to produce more forward peaked secondary
neutrons with lower energy. This would reduce the calculated leakage
multiplication and result in a value closer to those for ^{252}Cf in

the present experiment for the thicker beryllium shells. The relative number of neutrons in each of the four previously mentioned energy groups for ^{252}Cf in beryllium are listed in Table XV. As can be seen, all measurements result in leakage spectra which are harder than those from ^{252}Cf in polyethylene except for the 19.9 cm thick beryllium shell.

The ENDF/B-V/LANL cross sections underpredict the leakage multiplication for ^{252}Cf in the 4.6 cm shell while showing a trend similar to the measurements for the other shells. Again the leakage multiplication for the 13.8 cm and 19.9 cm shells are based on one-dimensional analyses with the entire thickness of beryllium included in the calculations. The calculated multiplication will probably increase for these configurations when the missing hemispherical shells are taken into account.

The second series of beryllium experiments was done to obtain information as to the adequacy of the (n,2n) representations in the theoretical cross sections. The experiments involved using DT neutrons in shells of 4.6 cm, 6.99 cm, 7.87 cm, 9.38 cm, 13.8 cm, and 19.9 cm of beryllium. A comparison of the calculated to measured neutron leakage multiplication is shown in Table XX. The calculations based on ENDF/B-IV predict the measured leakage multiplication quite well for the 4.6 cm to 9.43 cm thick beryllium shells while

TABLE XX

COMPARISON OF CALCULATED VERSUS EXPERIMENTAL (C/E)
LEAKAGE MULTIPLICATION FOR BERYLLIUM SHELLS WITH DT NEUTRONS*

Inner Radius (cm)	Shell Thickness (cm)	Multiplication				
		EXPERIMENT	B-IV **	C/E	B-V ***	C/E
8.00	4.6	1.43(.09)	1.28	0.90	1.32	0.92
3.17	6.99	1.50(.09)	1.41	0.94	1.46	0.98
20.06	7.87	1.56(.09)	1.52	0.97	1.55	0.99
3.17	9.43	1.46(.09)	1.55	1.06	1.61	1.10
8.00	13.8	1.50(.09)	1.83	1.22	1.84	1.23
8.00	19.9	1.52(.09)	2.09	1.38	1.97	1.30

The numbers in parentheses represent one standard deviation in the measurement uncertainty.

* - All calculated data represent 1-D modeling.

** - ENDF/B-IV

*** - ENDF/B-V/LANL

overpredicting the multiplication for the 13.8 cm and 19.9 cm shell thicknesses. Again note that the leakage multiplication for the 13.8 cm and 19.9 cm were calculated using one-dimensional analyses with the full thickness of beryllium used and are not directly comparable to the experimental results. The present data, although not directly comparable to the one-dimensional calculations or the previous experiments in which different geometries were used, indicates that the neutron multiplication properties of beryllium for shell thicknesses greater than 13.8 cm are overestimated in ENDF/B-IV.

Comparing the ENDF/B-V/LANL calculated leakage multiplication for DT neutrons with the present experimental results indicate that some revisions in cross sections have been made since ENDF/B-IV. The calculated leakage multiplication agrees with the measured leakage multiplication, within the 6% measurement uncertainty, for the 4.6 cm, 6.99 cm, 7.87 cm, and 19.9 cm thick beryllium shells. ENDF/B-V/LANL overpredicts the leakage multiplication for the 9.43 cm and 13.8 cm shells. The indication from the experiments is that the leakage multiplication versus the beryllium shell thickness is relatively flat for beryllium thicknesses between 9.43 cm and 19.9 cm. From these comparisons of the calculated versus the measured leakage multiplication it is obvious that the modifications made to ENDF/B-V by the Los Alamos National Laboratory are a step in the right direction; however, their full effect is not observed in the beryllium thicknesses used in this research. The revisions tend to increase the

multiplication for the thinner shells bringing them closer to the present measured values while decreasing the multiplication in the thicker shells.

Before applying these trends to the reevaluation of beryllium cross sections one needs to consider the two preliminary items. The above statements about the representations of the cross sections assume the experiment is viable and the calculations correctly model the experiment.[70] It has been demonstrated that the experimental technique is able to determine neutron leakage multiplication by measuring neutrons in the energy range of interest in the beryllium neutron multiplication experiments. There is a question; however, as to how well the experiments were modeled in the computations. It is felt, based on the fact that the effect of the reentrant hole has been shown to be negligible[4], that the beryllium assemblies with complete hemispherical shells are adequately modeled with one-dimensional calculations. The same cannot be said about the assemblies with missing hemispherical shells. To obtain information from these assemblies to compare with the experimental results would require multi-dimensional modeling. One way to do this would be to determine, with Monte Carlo, the neutron source distribution for input into the transport code. The actual source distribution may be more anisotropic with a preferential forward scatter than the experimental sweep with NE-213 indicated. It may also be necessary to model the

target assembly to determine its effect on the leakage multiplication.[71] The effect is not expected to be significant because the target assembly was made out of aluminum which is somewhat transparent to neutrons and no observable effects were seen when the leakage multiplication for the ^{252}Cf in the LLNL polyethylene sphere or the DT in the NCSU polyethylene sphere were measured. The most important item which could be more correctly modeled in either a two- or three dimensional code would be the effect of the missing hemispherical shells. Preliminary analyses using the two-dimensional code TRISM[72] suggests that the DT neutron leakage out the side of the beryllium shell assemblies which contain the void may be larger than the leakage from the side with solid beryllium.[70] This would imply that for DT neutrons the neutron leakage would be larger than that calculated by one-dimensional analysis with no voids taken into account.

In summary the ENDF/B-V/LANL DT calculated leakage multiplication for the beryllium shells of thickness 4.6 cm, 6.99 cm, and 7.87 cm, which are composed of complete shells, match that obtained from the present research. The calculated value for 9.43 cm, which is also composed of complete shells, is overpredicted by ENDF/B-V/LANL. The calculated leakage multiplication for the thicker beryllium assemblies with missing hemispherical shells is expected to decrease above that quoted in Table XX when more correctly modeled.

This will decrease the discrepancies between the ENDF/B-V/LANL calculations and the measured multiplication of the present research. The measured data for the beryllium shells of 9.43 cm to 19.9 cm thickness indicate that the leakage multiplication as a function of beryllium thickness is relatively constant whereas ENDF/B-V/LANL predicts an increasing response in the range used here. Based upon this further refinements of the ENDF/B-V/LANL cross sections may be warranted; however, insufficient calculated information is available to suggest qualitative changes in the cross sections for these thicker shells.

Chapter VII   Summary

A technique using Bonner spheres to measure neutron leakage multiplication has been developed, tested, and used to determine the neutron leakage multiplication from ^{252}Cf and DT neutrons in beryllium shells of thickness 4.6 cm, 6.99 cm, 7.87 cm, 9.43 cm, 13.8 cm, and 19.9 cm. The Bonner spheres with the associated response matrix (UTA4) and individual sphere correction factors were shown to precisely measure neutron leakage spectra from thermal to 14 MeV by comparing the measured leakage multiplication from polyethylene shells to calculated values. The use of a detector system with this extreme range of measurement capability allowed the experiments to be performed with a single detector system, simplifying the experiment and the resulting analyses.

The ^{252}Cf neutron source was chosen because it has a well characterized neutron energy distribution[4,22,37,38,52] and because it emits a major portion of its neutrons below the 2.68 MeV (n,2n) threshold of beryllium. The DT neutron source was chosen because its spectral shape is well known and because it represents neutrons found in a fusion reactor. The DT neutrons were produced with a neutron generator with a 150 keV accelerating potential. A target assembly containing an associated particle system was inserted into the shells via a reentrant hole. The associated particle detector was used to

normalize the DT neutron production and to monitor for DD neutron contamination.

All the beryllium assemblies were modeled with the one-dimensional discrete ordinates codes ANISN and ONEDANT with ENDF/B-IV and ENDF/B-V/LANL, respectively. A comparison of the leakage multiplication using ENDF/B-IV and ENDF/B-V/LANL indicated that some revisions have been made to ENDF/B-V/LANL to account for the secondary neutron distribution. This change has little effect on the calculated leakage multiplication for the thinner beryllium shells for the fissions neutrons from ^{252}Cf. This is expected because the total beryllium cross section was well characterized from thermal reactor criticality experiments and corrections to the energy-angle correlations have little effect on thin shell multiplication. A slight change was seen in the calculated multiplication for the thicker beryllium shells of 13.8 cm and 19.9 cm thicknesses. ENDF/B-V/LANL with its corrected energy-angle correlation produced more forward peaked secondary neutrons with lower energy reducing the calculated multiplication.

The ENDF/B-V/LANL revisions resulted in a higher leakage multiplication for DT neutrons in thin beryllium shells and lower leakage multiplication for shells thicker than 13.8 cm (2.42 MFP for DT neutrons). A study of the effect of the internal void radii with DT neutrons using ENDF/B-V indicated that neutron leakage

multiplication changes significantly with void radii for thick beryllium shells. Therefore, leakage multiplication cannot be directly compared between experiments unless they are of the same geometry.

A comparison of the calculated versus measured leakage multiplication for ^{252}Cf in beryllium indicates that for ENDF/B-IV the leakage multiplication for the 4.6 cm thick shell is underestimated whereas it is overestimated for the thicker shells. Because the beryllium assemblies of the 13.8 cm and the 19.9 cm shell thicknesses had missing hemispherical shells they could not be adequately modeled with one-dimensional calculations and the amount the calculations overpredict the leakage multiplication cannot be determined. The beryllium leakage multiplication predicted by ENDF/B-IV for the ^{252}Cf inside the thicker shells seems unrealistic. There appears to be no change in leakage multiplication with increasing thickness of beryllium. This is contrary to what one would expect for a neutron source which emits 66% of its neutrons below the (n,2n) threshold where the major portion of the reactions are either elastic scatter or absorbtion.

Comparing the ENDF/B-V/LANL ^{252}Cf-beryllium calculations with the measured leakage multiplication indicate that the revised cross sections are more closely aligned with the measurements than those from ENDF/B-IV. The difference in the multiplication for the 4.6 cm shell could indicates that either an additional revision in the

(n,2n) cross section or absorption cross section is needed in this
energy range. Before such a correction is made additional
measurements with beryllium thicknesses of the same order need to be
taken. The calculated multiplication for the 13.8 cm and 19.9 cm
shell thicknesses are not directly comparable with the measured
values, yet it is expected that the calculated multiplication for
these assemblies will increase if the void is taken into account.

A comparison of ENDF/B-IV DT-beryllium calculations with the
measured leakage indicates that for shell thicknesses between 4.6 cm
and 9.43 cm (0.8 to 1.64 MFP) there is good agreement. As shown in
previous experiments,[5,6,9,14,19] the calculations overpredict the
leakage multiplication for the thick beryllium shells.

The ENDF/B-V/LANL cross sections for DT neutrons tend to more
closely predict the measured leakage for the all the beryllium shells
when compared to ENDF/B-IV. Experimental results from the present
research indicate; however, that the neutron multiplication as a
function of beryllium thickness is relatively constant from 9.43 cm to
19.9 cm. Multi-dimensional calculations, to allow for the voids
created by the missing hemispherical shells, would be required to
obtain results directly comparable to the experimental multiplication
for the thicker shells before changes could be recommended to the
ENDF/B-V/LANL cross sections.

It is felt that the beryllium assemblies with complete hemispherical shells (4.6cm, 6.99 cm, 7.87 cm, and 9.43 cm thick beryllium assemblies) can be adequately represented by one-dimensional calculations. As such the ENDF/B-V/LANL ^{252}Cf calculated leakage multiplication agrees with the experimental data for all but the 4.6 cm shell and 19.9 cm shell. The ENDF/B-V/LANL DT calculated leakage agrees with the measured leakage multiplication for the 4.6 cm, 6.99 cm, and 7.87 cm thick beryllium shells with the results beginning to diverge at the 9.43 cm thickness. Direct comparison of the thicker beryllium assemblies with missing hemispherical shells would be meaningless without multidimensional analysis to include the reentrant hole, the target assembly, neutron source distribution, and the missing hemispherical shells. The ENDF/B-V/LANL DT calculated values indicate an overprediction for these thicker beryllium shells with the measured multiplication as a function of beryllium thickness being a fairly flat response between 9.43 cm and 19.9 cm.

APPENDIX A

TOTAL ERROR ASSOCIATED WITH BUNKI OUTPUT

The error quoted for the total fluence for BUNKI is based on how well the experimental data fit the BUNKI computed spectra. The uncertainty associated with each sphere (obtained from error propagation) was used only to weight the importance of the sphere data and was not propagated through BUNKI. To derive a realistic error associated with the total fluence, tests were performed with BUNKI. It was determined that the total fluence would vary by as much as 4% base upon the iteration scheme. In addition to this a 4% variation could be achieved by varying the initial input (this was a particular problem when beryllium shells were used). The errors for bare source spectra for the conditions above were less than 2% total. If the errors above are added in quadrature the resulting error of about 5.7% is obtained. It is felt that this error added in quadrature with the error obtained for a particular BUNKI run would give a good estimate of the uncertainty for a 68% confidence level on the multiplication.

APPENDIX B

EFFECTS OF D_2^+ CONTAMINATION

As stated in Chapter 3 the beam composition was determined using the technique described in Reference 23. The method is rather crude and provides only an estimate of the beam composition (a 30% uncertainty is associated with the values). The results for each target are shown below:

Target	D^+/D_2^+
#1	1.1
#2	1.9
#3	1.1

The effect of the D_2^+ component on the alpha normalization was determined by calculating the difference in the number of neutrons produced per alpha for 150 kV (D^+) versus 75 kV (D_2^+) and ratioing the number of neutrons produced assuming the entire pulse height peak is from D^+ to that produced by the correct number of D^+ and D_2^+. The discrepancy is largest for the case where the D_2^+ component is the largest. The error in the alpha normalization in this case is 1.7%.

APPENDIX C

CHOICE OF RESPONSE MATRIX

Of the six response matrices available for unfolding the
Bonner sphere data with BUNKI all but two were ruled out based upon
recommendation of T.L. Johnson. The two which were used were SAN4 and
UTA4.[50] As noted in Ref. 52 both response matrices fit a bare
^{252}Cf spectrum well while UTA4 predicts a total fluence less than
SAN4 for softer spectra (See Table below).

Average Energy from BUNKI(MeV)	Spectrum	SAN4	UTA4
0.3	Cf in 19.9-cm Be	0.91	0.67
0.8	Cf in 13.8-cm Be	1.1	0.93
1.3	Cf in 4.6-cm Be	1.26	1.22
2.0	Cf in 6.99-cm Be	1.1	1.0
2.5	DT in 19.9-cm Be	1.67	1.52
3.5	DT in 13.8-cm Be	1.54	1.5
4.1	DT in 9.4-cm Be	1.56	1.46
4.4	DT in 7.85-cm Be	1.66	1.56
5.0	DT in 6.99-cm Be	1.56	1.5
6.5	DT in 4.6-cm Be	1.43	1.43

The choice of the "correct" response matrix was based upon the one which came closest to the calculated leakage multiplication of a known material (obtained by placing ^{252}Cf in polyethylene spheres). The criteria for this investigation were: 1) simple geometry, 2) material of known cross section, 3) well characterized source with an emission of low energy neutrons where the largest discrepancies between response matrices occurs. Several tests were run with the results shown in Table XIII. Based upon this analysis UTA4 was chosen to more closely provide the correct leakage multiplication coming within 1% of the calculated value.

APPENDIX D

EFFECTS OF VARIATIONS OF "A"

Because the values for "A" used in the ESJ model were not recomputed for each set of measurements it was necessary to determine the effects of the uncertainty in "A" on the final beryllium neutron multiplication. Rather than tests each beryllium sphere combination (different neutron energy distributions) two cases were tested; 1) bare DT source and 2) DT in 3.5 mfp beryllium (70% of the neutrons had an energy less than 77 eV).

The values for A for the bare DT source and the DT in beryllium were those obtained from AmBe. If new values of A were recomputed their value would be lower for the bare DT source and larger for the DT in 3.5 mfp beryllium.

In each case the value for A was increased and decreased by a factor of 10. The change in the total fluence for each case relative to the total fluence obtained with the values of A from AmBe are shown below:

Source	Air Scatter	Effect
Bare DT	A X 10	-3.%
	A X 1/10	.3%
DT in 3.5 mfp Be	A X 10	.1%
	A X 1/10	.1%

To determine the maximum expected change in multiplication the total fluence in 3.5 mfp of beryllium obtained by increasing A by a factor of 10 was divided by the total fluence of the bare DT source obtained by decreasing A by a factor of 10. The resulting change was less than .5% when compared to the multiplication obtained with the values of A from AmBe. Therefore no extensive effort to determine new values for A for each spectrum was undertaken.

APPENDIX E

HUNT'S STABILITY CHECK

According to Hunt[21], to check the "internal consistency" of the measurements, the data must be analyzed by systematically varying the range of source-detector distances used as input to the various models. The slope and intercept were computed for all distances from D_1 to D_n, where D_1 is the minimum separation distance and D_n is the maximum separation distance, then reaccomplished for D_2 to D_n, then for D_3 to D_n, etc. If the least-squares' computed intercept and slope are stable for the range of measurement distances, then "both the measurements and method must be presumed correct".

To attempt to cover the entire spectrum of measurements, analyses were performed for a bare DT source and DT inside 3.5 mfp beryllium. Within these measurements a large and small Bonner sphere were chosen. The results are shown in Table E.1 and Table E.2. In each case the value for the intercept (C_0) and slope (RR) are shown with no points deleted (11 points used in the original data) along with their associated uncertainty. Shown below this are the values

for the intercept and slope with the specified number of points
deleted (the numbers in parentheses are the uncertainty associated
with these points using the t-distribution). In the column to the
right are the percent deviation of these values from the value with no
points deleted. In all cases analyzed the data satisfies the required
stability criteria.

TABLE E.1

HUNT'S STABILITY CHECK FOR THE 3.5 MFP BERYLLIUM WITH DT

# pts deleted	5.08 CM BONNER SPHERE		30.48 CM BONNER SPHERE	
	C_0 (%error) RR (%error)	% diff w/0 pts deleted	C_0 (%error) RR (%error)	% diff w/0 pts deleted
NONE	.085 (5.9)		.044 (3.1)	
NONE	.057 (4.3)		.008 (7.7)	
1.	.085 (7.6)	+0.7	.045 (3.8)	+0.5
1.	.057 (5.1)	-0.4	.008 (9.1)	-0.9
2.	.087 (9.9)	+2.7	.044 (4.8)	-1.2
2.	.056 (6.3)	-1.5	.008 (10.2)	+2.2
3.	.088 (13.2)	+4.0	.044 (6.3)	-1.7
3.	.056 (8.0)	-2.1	.008 (12.4)	+3.1
4.	.088 (18.7)	+3.7	.043 (8.6)	-3.1
4.	.056 (10.4)	-1.9	.008 (15.5)	+5.7
5.	.082 (29.4)	-3.1	.043 (12.2)	-2.2
5.	.058 (13.8)	+1.0	.008 (21.5)	+4.2
6.	.083 (48.2)	-2.5	.045 (19.0)	+1.8
6.	.058 (21.4)	+0.8	.008 (34.8)	-2.3
7.	.096 (87.)	+13.9	.047 (37.3)	+5.5
7.	.054 (45.)	-5.8	.007 (71.)	-8.2

TABLE E.2

HUNT'S STABILITY CHECK FOR BARE DT SOURCE

# pts deleted	20.32 CM BONNER SPHERE		30.48 CM BONNER SPHERE	
	C_0 (%error) RR (%error)	% diff w/O pts deleted	C_0 (%error) RR (%error)	% diff w/O pts deleted
NONE	.067 (3.4)		.080 (2.7)	
NONE	.019 (5.5)		.008 (11.5)	
1.	.067 (4.3)	+0.2	.081 (3.3)	+0.8
1.	.018 (6.4)	+0.3	.008 (13.5)	-2.7
2.	.067 (5.4)	+0.4	.081 (4.1)	+1.4
2.	.018 (7.6)	-0.5	.008 (15.9)	+4.6
3.	.066 (7.4)	-0.2	.081 (5.2)	+1.5
3.	.019 (9.6)	+0.1	.008 (19.5)	-4.9
4.	.068 (9.7)	+2.7	.081 (7.1)	+0.6
4.	.018 (12.6)	-3.2	.008 (15.5)	-2.1
5.	.067 (14.9)	+0.5	.080 (10.2)	+0.4
5.	.018 (17.3)	-0.3	.008 (32.1)	+0.9
6.	.068 (26.3)	+2.3	.082 (15.7)	+2.6
6.	.018 (30.1)	-2.5	.007 (52.0)	-7.8
7.	.075 (47.1)	+12.5	.086 (30.0)	+7.4
7.	.016 (62.3)	-12.5	.006 (116)	-21.0

APPENDIX F

RELATIVE NUMBER OF NEUTRONS PER ENERGY GROUP

To allow comparison of measured-unfolded spectra with
calculated spectra and to check the consistency of the calculated
leakage spectra with previous calculations the analyzed spectra were
binned into four energy bins corresponding roughly to the categories
chosen by Wong et al.[19] The categories chosen were 15-10 Mev,
10-2 MeV, 2 MeV - 0.77 eV, and less than 0.77 eV. As can be seen in
Table XV the relative number of neutrons leaking out of the sphere is
about the same between the calculated and measured unfolded spectra.

This information was also used to determine if a problem
existed with thermal neutron absorption in air. The ^{252}Cf in
polyethylene was used as the benchmark to determine whether the Bonner
sphere technique was valid. If the total fluence for this could be
accurately measured (with roughly 37% of the leakage occuring with an
energy less than 0.4 eV) then it was assumed that the total fluence
for measurements in beryllium spheres whose neutron energy
distribution was harder than the polyethylene could also be measured
with no concern of thermal absorption in air above that accounted for
in the air-scatter coefficient in the ESJ model.

APPENDIX G

MULTIPLICATION WITHOUT ROOM-RETURN SUBTRACTION

An investigation was performed to determine the amount of correction made for room-returned neutrons for DT neutrons inside the beryllium shells. The results are shown below in order of beryllium thickness. As can be seen the amount of room-return correction differs according to the energy of the leakage neutrons. Because of this and because the neutron leakage multiplication is determined by dividing the count-rate from neutron sources inside beryllium spheres by the count-rate from the source alone the multiplication obtained without first correcting the count-rate for room-returned neutrons is invalid.

Spectrum	Raw data @ 1 meter (n/cm2)	Room-return @ 1 meter (n/cm2)	% Correction for RR	Multiplication w/o RR correction
19.9-cm	1.245	0.444	36.0	1.70
13.8-cm	1.171	0.348	29.0	1.55
9.38-cm	1.201	0.335	28.0	1.61
7.87-cm	1.291	0.320	25.0	1.71
6.99-cm	1.192	0.337	28.0	1.60
bare DT	0.734	0.151	21.0	

APPENDIX H

VARIATION OF MULTIPLICATION WITH CENTER-LINE DISTANCE

An investigation was performed to determine the effect of variations in the measurement of the center-line distance between the source and the detector on the final multiplication value. This was accomplished by unfolding the count-rate at 1 meter from a bare ^{252}Cf measurement as taken in the lab then increasing the center-line distance 2-cm for each measurement location and again unfolding the spectrum. The change in the neutron fluence as obtained from BUNKI between these two measurements will be directly comparable to the change in neutron leakage multiplication that would result if a 2-cm variation in center-line distance was observed. The results are shown below:

Fluence at correct distance = 253.4 n/cm^2

Fluence at distance + 2-cm = 264.7 n/cm^2

Change in fluence @ 1 meter = 4.3% for 2-cm D_0 variation

REFERENCES

1. D.L. Smith, C.C. Baker, D.K. Sze, G.D. Morgan, M.A. Abdou, S.J. Piet, K.R. Schultz, R.W. Moir, and J.D. Gordon, "Overview of the Blanket Comparison and Selection Study," Fusion Technology 8, 10-44, (1985).

2. M.Z. Youssef and M.A. Abdou, "Uncertainties in Prediction of Tritium Breeding in Candidate Blanket Designs due to Present Uncertainties in Nuclear Data Base," Fusion Technology 9, 286-307, (1986).

3. S.A.W. Gerstl, D.J. Dudziak, and D.W. Muir, "Cross Section Sensitivity and Uncertainty Analysis with Application to a Fusion Reactor," Nuclear Science and Engineering 62, 137-156, (1977).

4. N.E. Hertel, "High-Energy Neutron Transport through Tungsten and Iron," Phd Thesis, University of Illinois at Urbana-Champaign (1979).

5. P. Cloth, D. Filges, R. Herzing, and N. Kirch, "Neutron Multiplication Effect of CTR Blankets Containing Beryllium," Proc. 9th Symposium on Fusion Technology, 569-575, (1976).

6. T.K. Basu, V.R. Nargundkar, P. Cloth, D. Filges, and S. Taczanowski, "Neutron Multiplication Studies in Beryllium for Fusion Reactor Blankets," Nuclear Science and Engineering 70, 309, (1979).

7. D.M. Drake, G.F. Auchampaugh, E.D. Arthur, C.E. Ragan, and P.G. Young, "Double-Differential Beryllium Neutron Cross Sections at Incident Neutron Energies of 5.9, 10.1, and 14.2 MeV," Nuclear Science and Engineering 63, 401, (1977).

8. M.Z. Youssef, R.H. Whitley, and D.H. Berwald, "Cross-Section Sensitivity Analysis for a Tandem Mirror Hybrid Reactor and Considerations Regarding New 9Be(n,2n) Cross Section Evaluations," Transactions Am. Nucl. Soc. 41, 75, (1982).

9. J.C. Doyle Jr. and J.D. Lee, "Monte Carlo Calculations of 14 MeV Neutron Multiplication in Thick Beryllium Assemblies and Comparison with Experimental Results," UCRL 89597, submitted to Nuclear Science and Engineering.

10. Ludlum Measurements Inc., Sweetwater Texas.

11. C.P.C. Wong, R.F. Bourque, E.T. Cheng, R.L. Creedon, I. Maya, R.H. Ryder, and K.R. Schultz, "Helium-Cooled Blanket Designs," Fusion Technology 8, 114-132, (1985).

12. R.W. Moir, J.D. Lee, C. Maniger, W.S. Neef Jr., A.E. Sherwood, D.H. Berwald, J.H. DeVan, I. Jung, "Helium-Cooled FLIBE Breeder Beryllium Multiplier Blanket," Fusion Technology 8, 133-148, (1985).

13. R.W. Moir, J.D. Lee, F.J. Fulton, F. Huegel, W.S. Neef Jr., A.E. Sherwood, D.H. Berwald, R.H. Whitley, C.P.C. Wong, J.H. DeVan, W.R. Grimes, and S.K. Ghose, "Design of a Helium-Cooled Molten-Salt Fusion Breeder," Fusion Technology 8, 465-473, (1985).

14. S.T. Perkins, E.F. Plechaty, and R.J. Howerton, "A Reevaluation of the 9Be(n,2n) Reaction and Its Effect on Neutron Multiplication in Fusion Blanket Applications," Nuclear Science and Engineering 90, 83-98, (1985).

15. Bulk Interim Reports 2-11, COPE-2338, -2514, -2532, -2576, -2752, -2753, COPP-726, -784, -816, Lawrence Livermore National Laboratory (1955-56).

16. "MORSE: A General Purpose Monte Carlo Multigroup Neutron and Gamma-Ray Transport Code," Radiation Shielding Information Center, Oak Ridge National Laboratory, CCC-127.

17. V.R. Nargundkar, T.K. Basu, O.P. Joneja, M.R. Phiske, and S.K. Sadavarte, "Neutron Multiplication Measurements in BeO for 14 MeV Neutrons," Fusion Technology 6, 93, (1984).

18. J.C. Doyle and J.D. Lee, Brush-Wellman N-50C Beryllium Specification, Appendix A UCID-20042, (1983).

19. C. Wong, E.F. Plechaty, R.W. Bauer, R.C. Haight, L.F. Hansen, R.J. Howerton, T.T. Komoto, J.D. Lee, S.T. Perkins, and B.A. Pohl, "Measurements and Calculations of the Leakage Multiplication from Hollow Beryllium Sphere," Fusion Technology 8, 1165-1173, (1985).

20. V.R. Nargundkar, T.K. Basu, and O.P. Joneja, "Re-Analysis of Neutron Multiplication Measurements in Thick Beryllium and Graphite Assemblies for 14 MeV Neutrons," submitted to Fusion Technology August 16, 1984.

21. J.B. Hunt, "The Calibration of Neutron Sensitive Spherical Devices," Radiation Protection Dosimetry 8, No4, 239, (1984).

22. A.B. Chilton, J.K. Shultis, R.E. Faw, Principles of Radiation Shielding, 78, Prentice-Hall, Inc., New Jersey, (1984).

23. H.M. Loebenstein and Y. Gazit, "A Simple Beam Charge Monitor for Neutron Generators," Nuclear Instruments and Methods 108, 387-388, (1973).

24. J. De Pangher and L.L. Nichols, "A Precision Long Counter for Measuring Fast Neutron Flux Density," BNWL-260 (1966).

25. H.W. Patterson and R. Wallace, "A Method of Calibrating Slow Neutron Detectors," UCRL-8359 (1958).

26. R.C. McCall and W.P. Swanson, "Neutron Sources and Their Characteristics," Proc. Conf. on Neutrons from Electron Medical Accelerators, NBS Spec. Publ. 554 (1979).

27. A.K. Savinskii and J.V. Filyushkin, "An Estimate of the Contribution by Neutrons Scattered in Enclosed Rooms to a Total Radiation Dose," Proc. Symp. on Neutrons Monitoring for Radiation Protection Purposes, IAEA, Vienna (1972), translated in UCRL-Trans-10771.

28. J. Csikai, "Use of Small Neutron Generators in Science and Technology," Preprint from Atomic Energy Review, Vol 11, No. 3, International Atomic Energy Agency, Vienna (1973).

29. D.T. Ingersoll, "Integral Testing of Neutron Cross Sections Using Simultaneous Neutron and Gamma-Ray Measurements," PhD Thesis, University of Illinois at Urbana-Champaign (1977).

30. R.L. Bramblett, R.I. Ewing, and T.W. Bonner, "A New Type of Neutron Spectrometer," Nuclear Instruments and Methods 9, 1, (1960).

31. N.E. Hertel and J.W. Davidson, "The Response of Bonner Spheres to Neutrons from Thermal Energies to 17.3 MeV," Nuclear Instruments and Methods in Physics Research A238, 509-516, (1985).

32. J.W. Davidson and N.E. Hertel, "An Equal Probility Neutron Detection System Using Bonner Spheres," Transactions of the American Nuclear Society 45, 609, (1983).

33. K.A. Lowry and T.L. Johnson, "Modification to Iterative Recursion Unfolding Codes to Find More Reasonable Neutron Spectra," draft NRL Memorandum Report (1983).

34. C.M. Eisenhauer, R.B. Schwartz, and T. Johnson, "Measurements of Neutrons Reflected from the Surfaces of a Calibration Room," Health Physics 42, 489, (1982).

35. C.M. Eisenhauer, J.B. Hunt, and R.B. Schwartz, "Calibration Techniques for Neutron Personal Dosimetry," Radiation Protection Dosimetry 10, No.1-4, 43-57, (1985).

36. J.B. Hunt, "The Calibration and Use of Long Counters for the Accurate Measurement of Neutron Flux Density," United Kingdom National Physical Laboratory, NPL-RS-5 (1976).

37. A. Gaines, personal communication (1986).

38. T.L. Johnson, Naval Research Laboratory, Washington D.C., personal communication (1986).

39. C.M. Eisenhauer, R.B. Schwartz, and R.C. McCall, "Effects of Air Scatter on Calibration of Instruments for Detecting Neutrons," submitted to Radiation Protection Dosimetry, (1987).

40. E.J. Axton, "The Effective Centre of A Moderating Sphere when used as an Instrument for Fast Neutron Flux Measurements," Journal of Nuclear Engineering 26, 581, (1972).

41. H. Ing and W.G. Cross, "Spectra and Dosimetry of Neutrons from Moderation of 235U and 252Cf Fission Sources in Water," Health Physics 29, 839, (1975).

42. L.R. Jones, "Diffuse Radiation View Factors Between Two Sphere," Journal of Heat Transfer, 422, (1965).

43. N. Juul, "Investigation of Approximate Methods for Calculation of the Diffuse Radiation Configuration View Factor Between Two Spheres," Letters in Heat and Mass Transfer 3, 513 (1976).

44. N. Juul, "Diffuse Radiation Configuration View Factors Between Two Spheres and their Limits," Letters in Heat and Mass Transfer 3, 205, (1976).

45. J.D. Felske, "Approximate Radiation Shape Factors Between Two Spheres," Journal of Heat Transfer 100, 547, (1978).

46. P.R. Bevington, Data Reduction and Error Analysis for the Physical Sciences, 56-65, McGraw-Hill Book Company, New York (1969).

47. J. Wolberg, Prediction Analysis, D. Van Nostrand Company, Inc., Princeton, New Jersey (1967).

48. S.A. McGuire, "A Dose Monitoring System for Neutrons from Thermal to 100 MeV," LA-3435, Los Alamos National Laboratory (1965).

49. R.S. Sanna, "Thirty-one Group Response Matrices for Multisphere Neutron Spectrometer over the Energy Range Thermal to 400 MeV," Health and Safety Laboratory, HASL-267 (1973).

50. G.E. Hansen and H.A. Sandmeier, "Neutron Penetration Factors Obtained by Using Adjoint Transport Calculations," Nuclear Science and Engineering 22, 315-320, (1965).

51. K. O'Brien, R. Sanna, and J.Laughlin, "Inference of Accelerator Stray Neutron Spectra from Various Measurements," CONF-651109, 286, (1965).

52. K.A. Lowry and T.L. Johnson, "The Effect of the Choice of Response Matrix on Unfolded Bonner Sphere Spectra, NRL Memorandum, (1984).

53. ENDF/B-V, compiled by R. Kinsey, "ENDF/B Summary Documentation," ENDF-201, BNL-NCS-17541, National Nuclear Data Center (1979).

54. K.M. Case, F. DeHoffman, and G. Placzek, Introduction to the Theory of Neutron Diffusion vol I, Los Alamos Scientific Laboratory (1953).

55. I. Carlvik, Nuclear Science and Engineering 30, 150, (1967).

56. R.E. Maerker, F.J. Muckenthaler, J.J. Manning, J.L. Hull, J.N. Money, K.M. Henry, and R.M. Freestone Jr., "Calibration of the Bonner Ball Neutron Detectors Used at the Tower Shielding Facility,", Oak Ridge National Laboratory, ORNL-TM-3465 (1971).

57. D. Nachtigall and G. Burger, "Dose Equivalent Determinations in Neutron Fields by Means of Moderator Techniques," Topics in Radiation Dosimetry, ed. F.H. Attix, Academic Press, New York (1973).

58. R. Gold, "An Iterative Unfolding Method for Response Matrices," Argonne National Laboratory, Argonne, Ill, ANL-6984 (1964).

59. R. Sanna, "Modification of an Iterative Code for Unfolding Neutron Spectra from Multisphere Data," Health and Safety Laboratory Energy Research and Development Administration, New York, HASL-311 (1976).

60. J. Doroshenko, S. Kraitor, T. Kuznetsova, K. Kushnereva, and E. Leonov, "New Methods for Measuring Neutron Spectra with Energy from 0.4 eV to 10 MeV by Track and Activation Detectors," Nuclear Technology 33, 296, (1977).

61. L. Brackenbush and R. Scherpelz, "SPUNIT, A Computer Code for Multisphere Unfolding," Computer Applications in Health Physics, Proc. of Health Physics Topical Meeting, Pasco, WA (1984).

62. T.L. Johnson personal communication (1987).

63. "ANISN: Multigroup One-Dimensional Discrete Ordinates Transport Code with Anisotropic Scattering," Radiation Shielding Information Center, Oak Ridge National Laboratory, CCC-254.

64. "ONEDANT: One-dimensional, Multigroup, Diffusion Accelerated, Neutral Particle Transport Code," Radiation Shielding Information Center, Oak Ridge National Laboratory, CCC-428.

65. R.J. Howerton and S.T. Perkins, "Evaluated Neutron-Interaction and Gamma-Ray Production Cross Sections of 9Be for ENDF/B-IV, BNL 17541 (1975).

66. DLC-31 DPL-1/FEWG1, ORNL/TM-4840, Radiation Shielding Information Center, Oak Ridge National Laboratory.

67. DLC-41/VITAMIN-C, ORNL-RSIC-37, Radiation Shielding Information Center, Oak Ridge National Laboratory.

68. D.J. Dudziak and J. Stepanek, "Los Alamos-EIR Co-operative work in the Field of Nucleonics and Particle Transport in Fusion Reactors for the Period of 1.7.1984-30.6.1986," Los Alamos Status Report, LA-UR-87-490, (1987).

69. "TRANSX-CTR: A Code for Interfacing MATXS Cross Section Libraries to Nuclear Transport Codes for Fusion Systems Analysis," Radiation Shielding Information Center, Oak Ridge National Laboratory, PSR-206.

70. J.W. Davidson, personal communication (1987).

71. R.C. Haight, personal communication (1987).

72. "TRISM: A Two-dimensional, Finite-element, Discrete-ordinates, Transport Code with Deterministic Streaming," by J.W. Davidson, B.A. Clark, D.R. Marr, and T.J. Seed.

VITA

Richard Steven Hartley, the son of Jimmie L. Hartley and
Fletcher Wilson Hartley, was born on August 31, 1954 in Houston,
Texas. In 1972, upon graduation from Governor Livingston Region High
School in Berkeley Heights, New Jersey, he entered Texas A&M
University. As an active member of the Texas A&M Corps of Cadets he
received an Air Force Scholarship in Physics while working part-time
at the Texas A&M Variable Energy Cyclotron. In May 1976 he received
a B.S. degree in Physics and was commissioned as an officer in the
United States Air Force. After graduation he was selected by the Air
Force as the only second lieutenant to receive an advanced degree in
nuclear engineering by attending the Air Force Institute of
Technology at Wright-Patterson AFB, Ohio. He graduated in March 1978
with a M.S. Degree in Nuclear Weapons Effects and was elected to the
Tau Beta Pi honor society.

He spent two tours of duty working for the Air Force
Technical Application Center (AFTAC) serving at McClellan AFB in
California and Eielson AFB in Alaska. His responsibilities in
California included the calibration and standardization of the
radiation detection equipment of the world-wide Atomic Energy
Detection System. While in Alaska he was responsible for directing

157

all the seismic, airborne, and nuclear detection operations of
AFTAC's largest detachment. For his efforts he was awarded the Air
Force Commendation Medal and the Meritorious Service Medal and he was
selected to return to the University of Texas to obtain his Ph.D. He
entered the University of Texas at Austin in September 1984. During
his stay he was elected as a member of the Phi Kappa Phi. His
follow-on assignment will be at the Headquarters of the Defense
Nuclear Agency in Alexandria, Virginia.

Permanent address: 11815 Chase Lake Dr
        Houston, Texas 77077

This dissertation was typed by Cathy Hartley.